

**Biochemical and biophysical investigation of the HalM2
lanthipeptide synthetase using mass spectrometry**

Journal:	<i>Canadian Journal of Chemistry</i>
Manuscript ID	cjc-2021-0124.R1
Manuscript Type:	Invited Review
Date Submitted by the Author:	04-Jun-2021
Complete List of Authors:	Hamry, Sally; McGill University Thibodeaux, Christopher; McGill University, Chemistry
Is the invited manuscript for consideration in a Special Issue? :	McGill
Keyword:	

SCHOLARONE™
Manuscripts

Biochemical and Biophysical Investigation of the HalM2 Lanthipeptide Synthetase using Mass Spectrometry

Sally R. Hamry and Christopher J. Thibodeaux*

Department of Chemistry
McGill University
801 Sherbrooke St. West
Montreal, QC, H3A 0B8

*to whom correspondence should be addressed

christopher.thibodeaux@mcgill.ca

1-(514)-398-3637

Abstract

The rapid emergence of antimicrobial resistance in clinical settings has called for renewed efforts to discover and develop new antimicrobial compounds. Lanthipeptides present a promising, genetically-encoded molecular scaffold for the engineering of structurally complex, biologically active peptides. These peptide natural products are constructed by enzymes (lanthipeptide synthetases) with relaxed substrate specificity that iteratively modify the precursor lanthipeptide to generate structures with defined sets of thioether macrocycles. The mechanistic features that guide the maturation of lanthipeptides into their proper, fully-modified forms are obscured by the complexity of the multistep maturation, and the large size and dynamic structures of the synthetases and precursor peptides. Over the past several years, our lab has been developing a suite of mass spectrometry-based techniques that are ideally suited to untangling the complex reaction sequences and molecular interactions that define lanthipeptide biosynthesis. This review focuses on our development and application of these MS-based techniques to investigate the biochemical, kinetic, and biophysical properties of the haloduracin β class II lanthipeptide synthetase, HalM2.

Keywords: lanthipeptides, biosynthesis, natural products, mass spectrometry, mechanistic enzymology

1. Introduction

Ribosomally synthesized and post-translationally modified peptides (RiPPs) are a class of natural products that have garnered significant interest due to their chemical structural diversity, range of biomedically useful activities, and their amenability to cell-based engineering approaches.¹⁻² RiPP biosynthesis begins with the transcription and translation of genes encoding for the RiPP precursor peptide and the associated biosynthetic enzymes (Figure 1A). Typically, the precursor peptide consists of an *N*-terminal leader peptide and a *C*-terminal core peptide. The leader peptide possesses recognition sequences that confer binding specificity to the biosynthetic enzyme(s) in the pathway, while the core peptide contains the sites of post-translation modification. Following enzymatic modification, often by enzymes that function iteratively at multiple sites, the mature peptide is exported from the producing cell and the leader peptide is proteolyzed, revealing the biologically active compound. The genetic encodability of both precursor peptide and biosynthetic enzyme(s), the structural modularity of the precursor peptide, and the relaxed substrate specificity of the biosynthetic enzymes are unique properties of RiPP systems that have inspired attempts to engineer RiPPs with novel functions.³⁻⁸ Moreover, using emerging bioinformatic tools,⁹⁻¹¹ the genetically encoded precursor peptides can be rapidly located in genome sequence data, and the structural novelty of the encoded RiPP can often be ascertained from the amino acid sequence of the precursor and the identities of the adjacent enzymes encoded in the gene cluster. This feature has led to an explosion of genome mining studies that have rapidly advanced this exciting field for novel natural product discovery.

Lanthipeptides are a large and structurally diverse group of RiPP natural products¹² that are widely dispersed across many bacterial phyla.¹³⁻¹⁴ Lanthipeptides possess a diverse range of biological activities such as antifungal,¹⁵ antiviral,¹⁶ cytotoxic,¹⁷ and morphogenic properties,¹⁸ as well as antiallodynic activity in mouse models of tactile neuropathic pain.¹⁹ However, most characterized lanthipeptides function as antibiotics against gram-positive bacteria. Structurally, lanthipeptides are characterized by the presence of thioether bridges (Figure 1B). These thioether rings endow the mature peptide with a macrocyclic structure that is critical for biological activity. The thioether moieties are installed into the precursor peptide (generically termed a LanA peptide) in a two-step reaction sequence (Figure 1B).¹² First, serine (Ser) and threonine (Thr) residues in the LanA core peptide are dehydrated to produce 2,3-didehydroalanine (Dha) and (*Z*)-2,3-didehydrobutyrine (Dhb), respectively. The second step involves an intramolecular Michael-type addition, where

Cys thiols in the core peptide add onto the nascent Dha/Dhb residues to generate lanthionine/methylanthionine (Lan/MeLan) rings, respectively.

Lanthipeptides are further subdivided into five phylogenetically distinct classes depending on the biosynthetic machinery that installs the (Me)Lan motifs (Figure 1C).²⁰⁻²¹ In class I lanthipeptide biosynthesis, separate enzymes catalyze dehydration (LanB)²² and cyclization (LanC).²³ In contrast, in the class II-IV lanthipeptides, a single multifunctional enzyme (LanM,²⁴ LanKC,¹⁹ or LanL,²⁵ respectively) catalyzes both dehydration and cyclization reactions. The biosynthetic mechanism of the recently discovered class V lanthipeptides has not yet been thoroughly examined.^{20, 26-27} The enzymes (or enzyme domains) responsible for lanthipeptide dehydration are phylogenetically divergent.²¹ LanB enzymes utilize glutamyl-tRNA^{Glu} as a substrate to catalyze dehydration via glutamylated peptide intermediates,²² whereas the LanM,²⁸ LanKC,²⁹ and LanL²⁵ enzymes catalyze dehydration via phosphorylated peptide intermediates in an ATP- or GTP-dependent process. Moreover, the LanM enzymes catalyze phosphoryl transfer and elimination in the same active site,³⁰ whereas the LanKC, and LanL enzymes utilize distinct kinase and lyase subdomains (Figure 1C). The cyclase enzymes involved in thioether bridge formation in all classes of lanthipeptides are structurally related to each other and to protein farnesyltransferases,^{21, 23} a group of enzymes that also catalyze alkylation of thiol moieties.³¹⁻³² The class I, II, and IV cyclases are Zn²⁺ metalloenzymes. The cyclase domains of the class III synthetases lack the conserved Zn ligands and do not bind to metal ions.³³ Intriguingly, LanKC enzymes are also functionally divergent and install the bicyclic labionine residue (Figure 1D).¹⁹

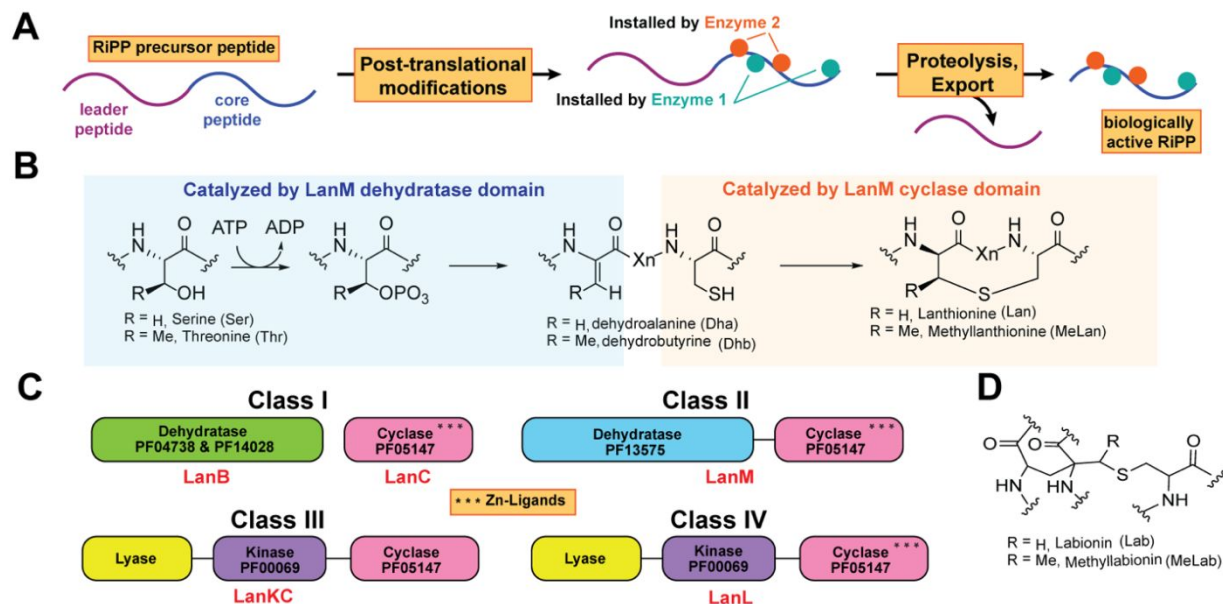


Figure 1. General features of RiPP and Lanthipeptide Biosynthesis. A) RiPPs are genetically encoded peptides partitioned into an *N*-terminal leader and a *C*-terminal core. The core peptide is modified (often iteratively) by enzymes with relaxed substrate specificity. Proteolysis and export from the cell typically complete the biosynthetic pathway. B) Chemical mechanism of class II lanthipeptide synthetase (LanM) enzymes, involving ATP-dependent dehydration of Ser/Thr residues, followed by Michael-type addition to form the thioether bridges. C) The four characterized classes of lanthipeptide synthetases. The pfam identifier for each structurally conserved domain is provided. The asterisks in the cyclase domain denote the presence of conserved Zn ligands, which are absent in the class III cyclase. D) The structure of the bicyclic (methyl)labionine residues produced by class III lanthipeptide synthetases.

A remarkable feature of lanthipeptide biosynthesis is the ability of the biosynthetic machinery to install a specific set of thioether rings into a given LanA precursor peptide. This biosynthetic fidelity is critical for producing final macrocyclic products that retain biological activity. Both dehydration and cyclization reactions are strongly exergonic,³⁴⁻³⁵ raising questions as to how the dehydration and cyclization activities of lanthipeptide synthetases are coordinated in time and space to generate specific thioether topologies with minimal production of biologically inactive side products. This conundrum extends more generally to many other enzymes involved in RiPP biosynthesis, which must somehow balance their inherently relaxed substrate specificities with the demands of biosynthetic fidelity in order to maintain the biological functions of their products. Biochemical studies of lanthipeptide synthetases have shown that the precursor peptide

sequence,^{21, 36} the identity of the Zn ligands in the cyclase active site,³⁷ and the relative kinetics of dehydration/cyclization³⁸⁻³⁹ all play roles in defining biosynthetic fidelity (albeit to different extents in different enzymes/systems).

This review will focus on efforts by our group to define the biochemical and biophysical factors that contribute to function and fidelity in class II lanthipeptide synthetases (LanM enzymes). We begin the review with an historical perspective of *in vitro* studies on LanM enzymes (Section 2), not only to introduce the most salient mechanistic and structural features of the system, but also to contextualize the knowledge gaps that have motivated development of new tools to study these systems (outlined in Sections 4-6). In Section 3, we briefly introduce the haloduracin β synthetase (HalM2) and its substrate peptide (HalA2) from *Bacillus halodurans* as a model system for elucidating structure-function relationships in class II lanthipeptide synthetases. Sections 4-6 highlight our systematic and detailed investigations into the HalM2:HalA2 system,^{38, 40-43} and illustrate the many powerful and unique advantages of high-resolution mass spectrometry (MS) for characterizing the mechanisms of lanthipeptide biosynthesis. Namely, MS-based methods can assess every level of protein/peptide structure – all of which are relevant to understanding the mechanisms of lanthipeptide biosynthesis. Section 4 discusses MS-based kinetic assays combined with tandem mass spectrometry to map post-translational modification regiochemistry and to define the preferred sequence of reactions leading to maturation of the HalA2 precursor peptide. In Section 5, we detail the use of hydrogen-deuterium exchange mass spectrometry (HDX-MS) to probe conformational dynamics in local secondary structural elements of HalM2 and to study how these dynamics are influenced by ligand binding and mutagenesis. In Section 6, we employ native ion mobility mass spectrometry (IM-MS) to profile the tertiary structure and conformational landscapes of natively folded HalM2 and its non-covalently bound complex with HalA2. Finally, we conclude with a brief outlook on the role that MS-based techniques will continue to play in the investigation of lanthipeptide and RiPP biosynthesis.

2. Biochemical and structural studies elucidate basic features of LanM catalysis

The lactacin 481 synthetase (LctM) from *Lactococcus lactis* was the first class II lanthipeptide synthetase to be characterized *in vitro*.²⁴ This enzyme catalyzes the four-fold dehydration of LctA and the installation of three interlocked thioether rings (Figure 2A). Early studies on LctM established that ATP was required for activity and that phosphorylated peptide intermediates were

generated during turnover with truncated LctA analogues, consistent with a dehydration mechanism involving a phosphorylation-elimination reaction sequence.²⁸ Subsequent *in vitro* studies of a large number of LanM enzymes have confirmed their ubiquitous dependence on ATP for activity.¹² The absence of detectable phosphopeptide intermediates with the native LctA substrate suggested that the phosphorylation and elimination reactions are normally strongly coupled. Structural studies (*vide infra*) have confirmed that both phosphorylation and elimination occur within the same active site.³⁰ Multiple amino acid sequence alignments revealed sets of invariant amino acid residues in LanM enzymes that were subsequently mutated and shown to play essential roles in dehydration⁴⁴ and cyclization catalysis.⁴⁵ The involvement of these residues in the chemical mechanisms of dehydration and cyclization are discussed below in the context of the CylM crystal structure (Figure 2C-D).³⁰ Finally, several studies investigated the role of the LctA leader peptide in directing the post-translational modifications installed by LctM.^{39, 46-48} Introduction of proline residues into the leader peptide was strongly detrimental to activity, perhaps disrupting putative α -helical structure in the leader.⁴⁶ Studies using separate leader and core peptide molecules provided to LctM *in trans* provided strong evidence for a leader peptide induced allosteric activation of LctM.⁴⁸ Namely, the minimal LctM dehydration activity on the isolated core peptide was substantially enhanced in the presence of the leader peptide. Interestingly, translational fusion of the LctA leader peptide to the *N*-terminus of LctM produced a constitutively active LctM variant enzyme that efficiently processed free LctA core peptides containing non-proteinogenic amino acids.⁴⁷ On the basis of these data, a conformational selection model was proposed for the leader peptide-dependent activation of LctM.

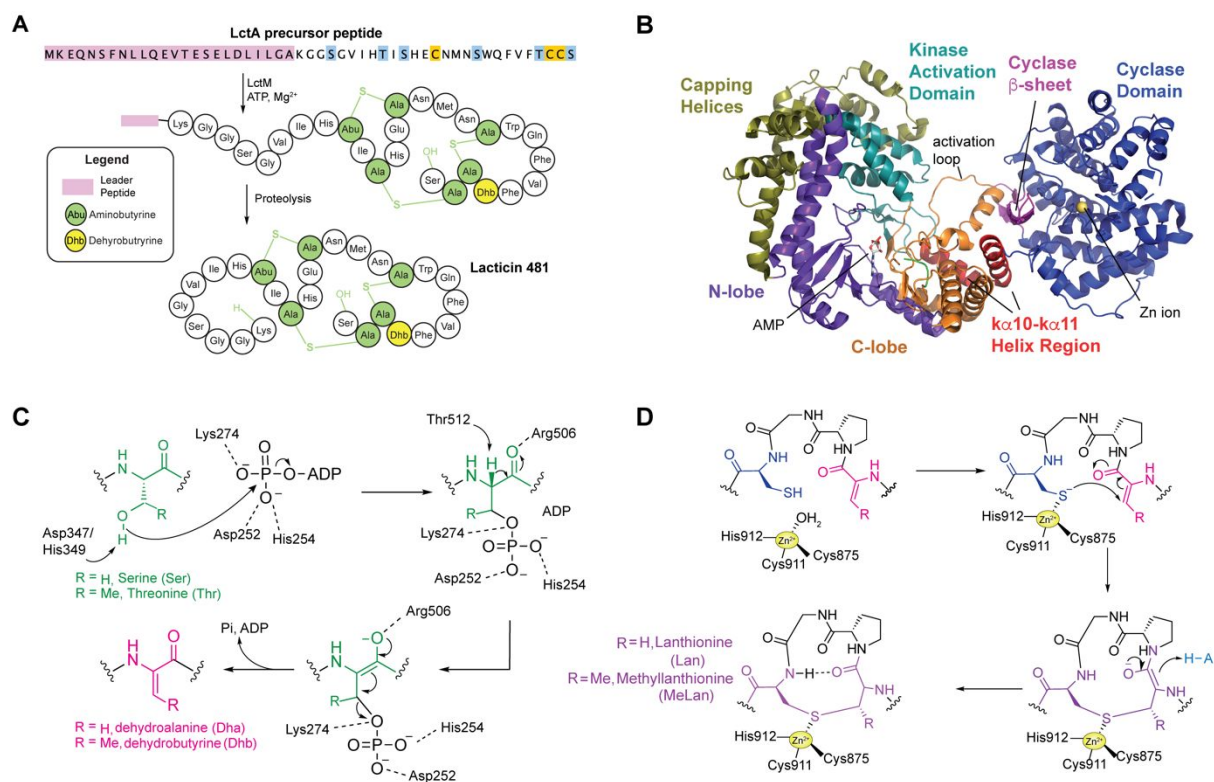


Figure 2. Early biochemical and structural studies of class II lanthipeptides. A) Structure of lacticin 481, produced from LctA by LctM. B) X-ray crystal structure of CylM using the subdomain nomenclature proposed by Dong et. al.³⁰ Putative chemical mechanisms for dehydration (panel C) and cyclization (panel D) catalyzed by CylM. All of the catalytic residues shown in panels C and D are absolutely conserved in LanM enzymes.

Deeper insight into the chemical mechanism of class II lanthipeptide synthetases was achieved when the 2.2 Å resolution X-ray crystal structure of the CylM enzyme from *Enterococcus faecalis* was solved.³⁰ Consistent with the earlier mutagenesis studies, the structure revealed two distinct domains: an *N*-terminal dehydration domain and a *C*-terminal cyclization domain (Figure 2B). Despite lacking detectable amino acid sequence similarity with proteins of known function, the *N*-terminal dehydratase domain is structurally homologous to the catalytic core of lipid kinases. This observation is consistent with the proposed mechanism of dehydration for LanM proteins involving ATP-dependent phosphorylation of Ser/Thr residues followed by phosphate elimination. In addition to the *N*- and *C*-lobe domains characteristic of lipid kinases, the CylM dehydratase domain contains several unique structural elements. These include the “capping helices” and the kinase activation domain (KA), the latter of which interacts with an unusually well-organized

kinase activation loop. The KA domain supplies catalytic residues (Arg506 and Thr512 in CylM) that facilitate the phosphate elimination step. The catalytic residues involved in phosphoryltransfer and elimination are all appropriately clustered in the active site to carry out their proposed roles in catalysis (Figure 2C). As expected on the basis of sequence homology, the CylM cyclization domain possesses the α/α -barrel fold found in the class I lanthipeptide nisin cyclase, NisC,²³ which encapsulates a single Zn^{2+} ion coordinated by Cys875, Cys911, His912. The fourth Zn^{2+} coordination site is accessible for binding to precursor peptide Cys thiols from the surface of the enzyme. Following Michael-type addition (Figure 2D), the incipient $C\alpha$ anion is likely protonated by His835, which is conserved in LanM enzymes and was shown to affect cyclization catalysis by LctM⁴⁵ and H/D exchange at $C\alpha$ in the precursor peptide substrate of HalM2.⁴⁹ A 3-stranded antiparallel β -sheet in the cyclase domains forms the majority of the interface with the *N*-terminal dehydratase domain via interactions with the dehydratase $k\alpha 11$ helix. As shown below in the context of HalM2, the LanM structural fold – in particular the interface between the dehydratase and cyclase domain – is dynamic and highly sensitive to ligand binding.

3. Discovery and preliminary characterization of the haloduracin biosynthetic gene cluster

Haloduracin – a two-component lanthipeptide produced by *Bacillus halodurans* C-125 – holds a noticeable place in the history of natural product biosynthesis as the first example of a biologically active natural product to be discovered using a bioinformatic genome-mining based approach (Figure 3).⁵⁰ The haloduracin biosynthetic gene cluster encodes for two precursor peptides (HalA1 and HalA2), two class II lanthipeptide synthetases (HalM1 and HalM2), and a bifunctional protease-transport protein (HalT).⁵⁰ *In vitro* reconstitution of this system showed that while a small amount of cross-reactivity exists, HalM1 selectively modifies the HalA1 precursor peptide and HalM2 selective processes the HalA2 peptide.⁵¹⁻⁵² HalM1 dehydrates HalA1 three times and installs three thioether rings, whereas HalM2 dehydrates HalA2 seven times and installs four thioether rings. In both precursor peptides, a single dehydratable residue in the core peptide escapes modification. Agar disk diffusion assays using a *Lactococcus* reporter strain demonstrated that the fully modified and proteolyzed Hal α and Hal β peptides function synergistically as a potent two-component antibiotic with a minimum inhibitory concentration of 40 nM.⁵⁰⁻⁵¹ The mode of action involves binding of Hal α to the lipid II intermediate of peptidoglycan biosynthesis in a 2:1 stoichiometry, which inhibits cell wall biosynthesis.⁵³

Subsequent binding of two equivalents of Hal β is believed to form pores in the bacterial plasma membrane leading to rapid depolarization and cell death. Importantly, the HalA2 precursor peptide is much more soluble in buffered aqueous solution than the LctA precursor peptide. For this reason, the HalM2:HalA2 system has proven to be a much more tractable system for quantitative *in vitro* measurements.

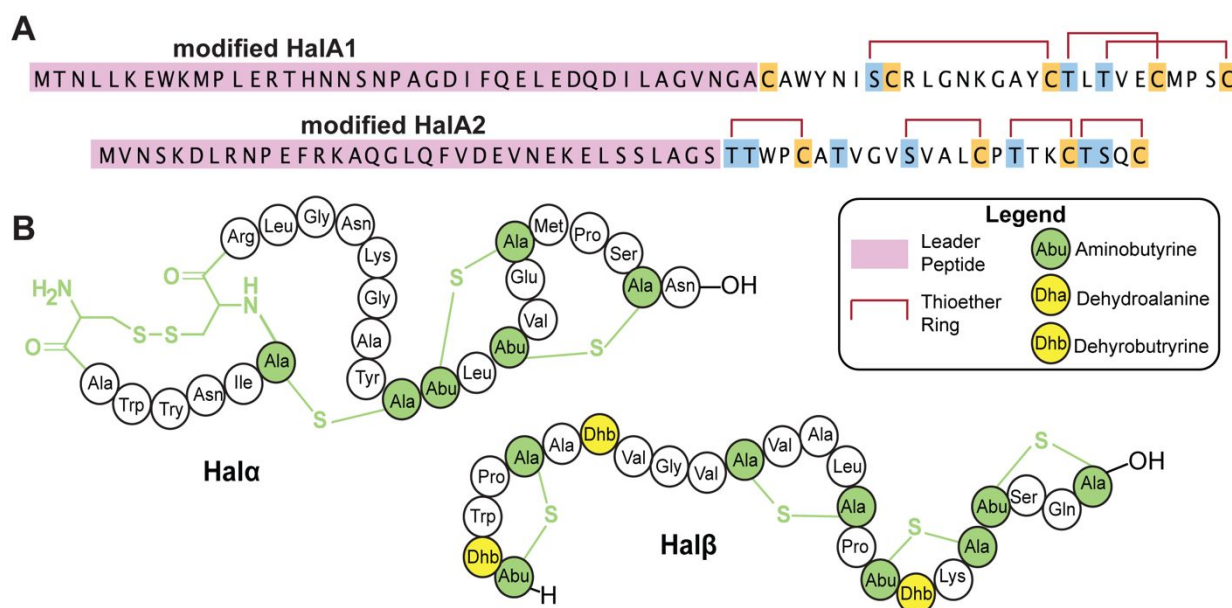


Figure 3. Biosynthesis of the Two-Component Lanthipeptide, Haloduracin. A) The HalA1 and HalA2 precursor peptides are modified by HalM1 and HalM2, respectively. B) Following proteolytic cleavage of the leader peptides and cellular export by HalT, the Hal α and Hal β peptides function synergistically to inhibit cell wall biosynthesis and to permeabilize the plasma membrane of gram-positive bacteria.

4. Developing mass spectrometry-based methods to profile HalM2 reactivity

The multifunctional nature of LanM enzymes presents challenges for detailed mechanistic investigation because multiple LanA-derived intermediates are typically produced simultaneously under *in vitro* conditions, generating highly complex reaction mixtures. Mass spectrometry provides an ideal solution to this problem because following alkylation of free cysteine thiols in the core peptide, each type of LanM-catalyzed post-translational modification results in a mass change. The number of each type of modification can then be rapidly inventoried from the m/z values of the LanA intermediates. Moreover, individual peptide ions can be fragmented in the

gas phase to establish the regiochemistry of each post-translational modification within the core peptide. If the reaction mixture is sampled as a function of time, detailed biosynthetic pathways can be constructed for the LanM-catalyzed sequence of reactions using a single analytical platform with high sensitivity and reproducibility.

The timing and order of modifications catalyzed by HalM2 was first assessed using Fourier transform ion cyclotron resonance (FTICR) mass spectrometry.⁵⁴ This study was the first to show the impressive catalytic efficiency of HalM2, which successfully installed the native set of seven dehydrations and four thioether rings into HalA2 in a matter of minutes under the *in vitro* conditions used. Tandem mass spectrometry studies of partially modified intermediates using collision induced dissociation (CID) revealed two interesting features of HalM2 catalysis. First, dehydration and cyclization occurred on similar time scales, suggesting that the HalA2 core peptide undergoes multiple binding and dissociation events to each active site of HalM2 during peptide maturation. The active sites of the dehydratase and cyclase domains are separated by approximately 40 Å (Figure 2B). Thus, this data provided indirect evidence for a highly conformationally dynamic HalM2:HalA2 Michaelis complex and hinted at a possible mechanism for biosynthetic fidelity control. Namely, by staggering the production of Dha/Dhb residues with the installation of thioether rings, the number of potential thioether ring isomers that can be installed by the HalM2 cyclase domain is drastically reduced. Second, the dehydrations were installed in a directional manner from the *N*-terminus to the *C*-terminus. Subsequent work has revealed that many LanM enzymes (as well as other lanthipeptide synthetases) exhibit directionality in the order of dehydrations and/or cyclizations.^{38-39, 55} Curiously, however, this directionality differs from system to system, arguing against the involvement of conserved conformational motions in establishing directionality and instead favoring a model governed by factors specific to each system, perhaps involving different enzyme:peptide intermolecular interactions and the intrinsic structural propensities of the precursor peptides.

In these initial mechanistic studies of HalM2, no attempt was made to quantify the time-dependent changes in the relative concentrations of the various HalA2 reaction intermediates. A robust kinetic assay would enable more detailed investigation into the mechanistic features that govern lanthipeptide maturation. Moreover, comparisons of kinetic properties between different LanM enzymes may provide insight into the observed functional heterogeneity of these systems (*e.g.* their differences in directionality, catalytic efficiency, and substrate specificity). Building on earlier

work by Kelleher and co-workers,⁵⁶⁻⁵⁷ we developed a semi-quantitative liquid chromatography electrospray ionization mass spectrometry (LC-ESI-MS) based assay to profile the steady state kinetic parameters of LanM enzymes (Figure 4).³⁸ In this approach, aliquots from HalM2:HalA2 reaction mixtures are acid quenched, reduced and alkylated (to reveal free Cys thiols), desalted using solid phase extraction, then analyzed by LC-ESI-MS. Importantly, the LC-ESI-MS analysis is performed on the intact HalA2 precursor peptide. The relatively large size of HalA2 (~8883 Da), coupled with the insignificant mass change associated with the post-translational modifications, ensures that the ionization properties of the various HalA2 intermediates in the ESI source are similar.³⁸ Thus, the intensities of the MS-detected peptide ion signals are proportional to peptide concentration, enabling highly robust relative quantitation where the fractional abundance of each HalA2-derived intermediate in the reaction mixture can be determined from the total signal (*e.g.* the sum of the ion intensities for all intermediates). Moreover, the ESI process generates different charge states of each peptide intermediate, effectively allowing for multiple measurements of the fractional abundance for each peptide in every LC-ESI-MS sample. Finally, we employed numerical simulation approaches to globally fit the kinetic data to biosynthetic models, allowing us to extract net rate constants for the individual chemical transformations in the multi-step LanM-catalyzed reaction. This approach generates highly reproducible kinetic data across different protein preparations, MS instruments, and researchers.^{38, 40, 42}

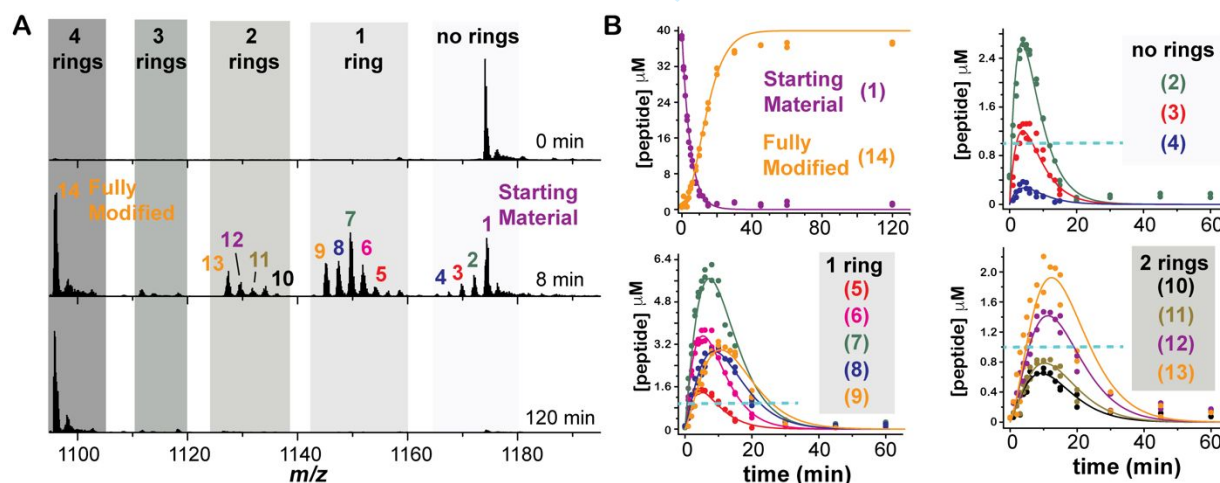


Figure 4. LC-ESI-MS based kinetic analysis of HalM2. A) Mass spectral time course for the HalM2-HalA2 reaction (the 8⁺ ions are shown). Compounds 1-14 represent HalA2 intermediates that differ in the number of dehydrations and thioether rings. Similar signals were observed for the 6⁺ to 10⁺ charge states. B) The fractional abundance of HalA2 intermediates were determined from the ion signals in panel A and were fitted globally to the kinetic model shown in Figure 5

using numerical simulation. The dashed blue lines indicate the 1 μM concentration of HalM2 used in the assay, clearly showing that most intermediates are released from the enzyme and accumulate prior to further processing. Data have been reproduced with permission from reference 38.

This semi-quantitative MS-based kinetic approach revealed many interesting functional properties of HalM2 (Figures 4 and 5). First, the concentrations of many of the HalA2 intermediates generated in the reaction accumulate to levels that exceed the concentration of HalM2 used in the assay, suggesting that HalM2 installs modifications in a distributive kinetic mechanism where the dissociation rates of the HalA2 intermediates are competitive with the rates of forward modification. Nevertheless, certain intermediates (such as HalA2 species containing three thioether rings, Figure 4) do not accumulate, suggesting that these species are very efficiently converted into more advanced biosynthetic intermediates prior to dissociating from the enzyme. That is to say, segments of the reaction sequence follow a processive kinetic mechanism. The analysis also revealed the existence of parallel reaction pathways (Figure 5), reinforcing the notion that the dehydratase and cyclase activities of HalM2 are kinetically competitive and occur on similar time scales. Interestingly, the kinetic simulations suggested that the presence of Dha/Dhb residues in the HalA2 core peptide could affect the rates of cyclization. Similarly, the presence of thioether rings could influence the rates of Ser/Thr dehydration. This data provided the first direct evidence that the structure of a maturing RiPP precursor peptide could directly impact the kinetics of downstream modifications, providing a mechanism by which specific sets of post-translational modifications are installed in an orderly (directional) process. Finally, following the formation of the second thioether ring (which represented the slowest overall step in the entire pathway), the final two thioether rings were very efficiently installed, suggesting that intermolecular interactions between HalM2 and HalA2 may be changing during maturation in a manner that facilitates more efficient docking and modification of the peptide in the cyclase active site.

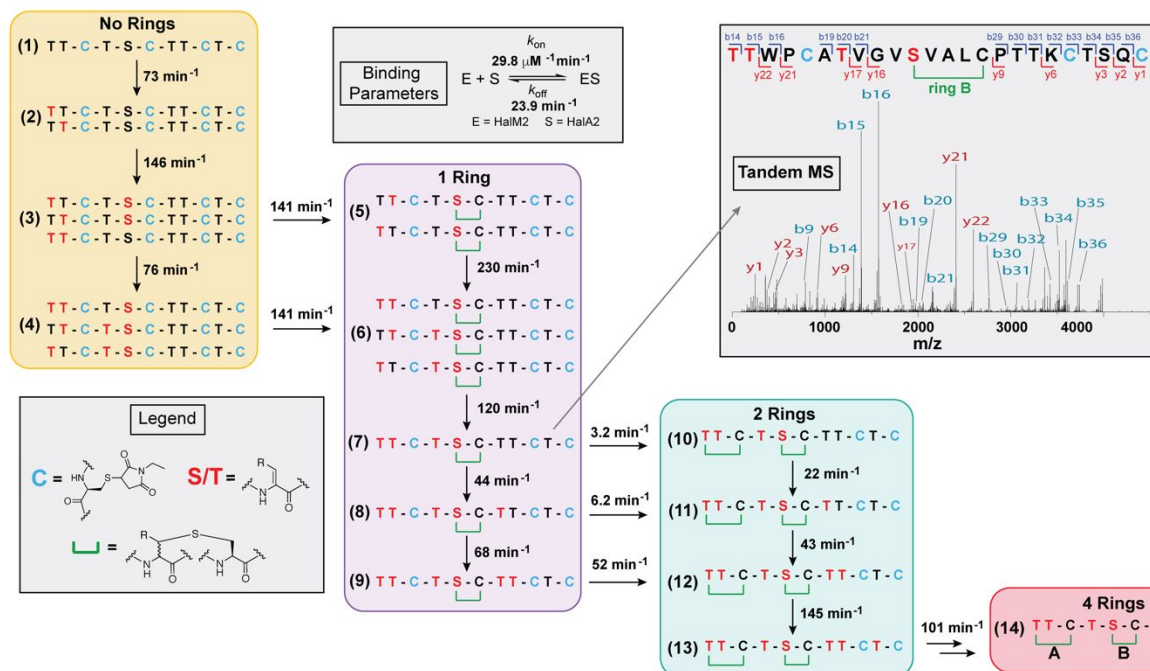


Figure 5. Biosynthetic model for HalM2.^{38, 42} For simplicity, only the Ser/Thr/Cys residues in the HalA2 core peptide involved in the post-translational modifications are shown. The simulated kinetic data from Figure 4 permitted the development of a detailed biosynthetic model for the HalM2-HalA2 reaction. Tandem MS fragment ion analysis of reaction intermediates (shown here for intermediate 7) allowed the dehydration and cyclization regiochemistry to be determined.⁴² Several constitutional isomers were distinguishable for compounds 2-6, indicating that the dehydration order is not strict, though there is a general preference for an *N*- to C-terminal directionality. The cyclization order was ring B → A → C/D. Tandem MS data have been reproduced with permission from reference 42.

Comparison of the kinetic properties of HalM2 with the properties of the prochlorosin synthetase (ProcM) from *Prochlorococcus* MIT9313 revealed additional interesting differences.³⁸ Unlike most LanM enzymes (such as HalM2) that process a single LanA precursor into a single final product, ProcM naturally accepts a small library of 30 different prochlorosin precursor peptides (Figure 6A) and generates post-translationally modified products with numerous different thioether ring topologies (Figure 6B).⁵⁸ As perhaps expected, kinetic analysis revealed that this naturally relaxed substrate specificity of ProcM comes at a cost of reduced catalytic efficiency (Figure 6D).³⁸ First, ProcM generates phosphorylated ProcA2.8 intermediates (Figure 6C), suggesting that the phosphoryltransfer and elimination steps are not strongly coupled in this enzyme. This stands in stark contrast to HalM2 and LctM, which do not generate detectable quantities of phosphorylated

intermediates with wild type substrates. Another striking difference between the kinetic properties of HalM2 and ProcM was found in the rates of thioether ring formation. Whereas the cyclization rates in the HalM2:HalA2 system increased as the HalA2 precursor matured towards the final product, the rate of the final cyclization in the ProcM:ProcA2.8 system decreased dramatically relative to the rate of the first cyclization. Thus, HalA2 intermediates become better substrates for cyclization as the precursor peptide acquires structure (thioether rings) while ProcA2.8 intermediates become worse substrates as thioether rings are installed. The hypothesis that emerges from this data is that the catalytically efficient enzyme, HalM2, has evolved specificity for the thioether topology found in the Hal β final product. In contrast, the flexible and inefficient enzyme, ProcM, which generates a number of distinct thioether topologies in its substrates, has apparently not evolved specific interactions for partially cyclized core peptides that might be useful for increasing catalytic efficiency.

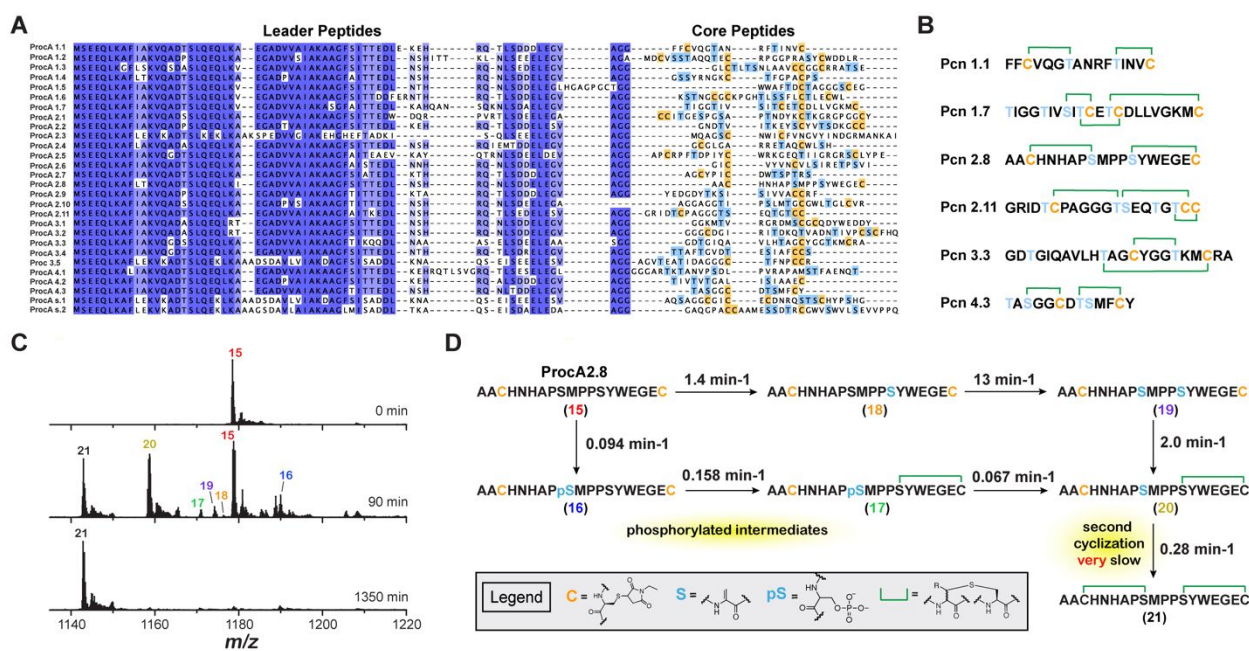


Figure 6. The promiscuous prochlorosin synthetase (ProcM) accepts 30 different ProcA precursor peptides as substrates.⁵⁸⁻⁵⁹ A) The ProcA peptides have a highly conserved leader sequence and a hypervariable core. B) ProcM installs different thioether topologies into the ProcA precursor peptides.⁶⁰ C) ESI mass spectral time course of the ProcM-ProcA2.8 reaction, showing the presence of phosphorylated intermediates (species 16 and 17). D) Numerical simulation of the kinetic data extracted from panel C.³⁸ In contrast to the highly efficient late stage cyclizations in

the HalM2-HalA2 system, the final cyclization (20 → 21) is the rate-limiting step in the ProcM-ProcA2.8 system. Data in panel C have been reproduced with permission from reference 38.

Cumulatively, the kinetic data on HalM2 and ProcM are consistent with a mechanistic model where enzyme:peptide interactions – which change in time as the LanA precursor acquires post-translational modifications – play a key role in defining the kinetic parameters measured in the steady state and, ultimately, the preferred pathway for the multistep maturation (Figure 7). The model proposes that core peptide docking equilibria into the dehydratase/cyclase active sites is a stochastic process that can be influenced by the set of modifications present in the peptide. This model can account for the observed alteration in dehydratase/cyclase activities, the fact that dehydration/cyclization rates for specific modifications depend on the post-translational modification state of the peptide, and the observation that HalM2 and ProcM have very different catalytic efficiencies for late-stage cyclization reactions. In addition, differences in LanA peptide binding mode might explain why some LanMs (such as HalM2 and LctM) install modifications in an *N*- to *C*-terminal direction, while others (such as ProcM) install modifications in an ordered pattern but with less stringent control over directionality.

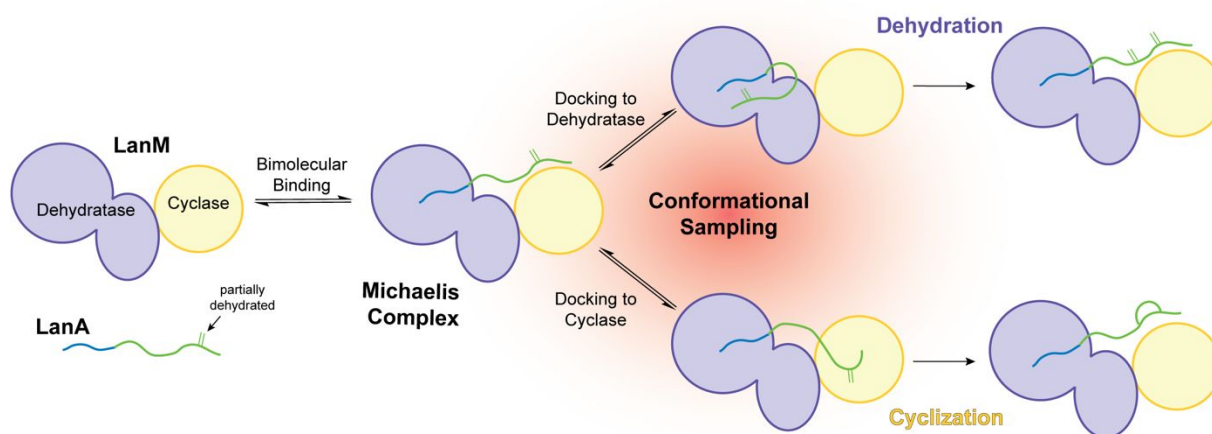


Figure 7. Conformational sampling model for HalM2 catalysis involving kinetically significant docking interactions between the core peptide and the dehydratase/cyclase active sites.

5. Probing functional conformational dynamics in HalM2 with hydrogen-deuterium exchange mass spectrometry (HDX-MS) and site directed mutagenesis

The kinetic studies provided several lines of evidence that conformational processes in the LanM:LanA Michaelis complex play a critical role in mediating the sequence of biosynthetic events. To better understand the role of protein-peptide interactions and conformational changes in LanM systems, direct measurements of these biophysical processes are needed. However, LanM enzymes have remained notoriously recalcitrant to characterization by traditional structural biology approaches such as X-ray crystallography and NMR spectroscopy. The X-ray crystal structure of the peptide-free CylM enzyme discussed above remains the only high-resolution LanM structure reported to date.³⁰ Several features of class II lanthipeptide systems have likely contributed to the dearth of structural information in the literature. First, as shown below, many LanM enzymes are likely structurally dynamic, which is expected to make X-ray crystallography difficult. Second, LanM enzymes are large (typically > 100,000 Da), which leads to poor signal dispersion in NMR data and makes spectral assignments difficult. Third, precursor lanthipeptides are also large and intrinsically disordered, making structural studies of LanM-LanA complexes challenging.

We reasoned that hydrogen-deuterium exchange mass spectrometry (HDX-MS) would provide a highly versatile and sensitive platform for illuminating functionally relevant biophysical processes in LanM (and other RiPP) biosynthetic enzymes. HDX-MS quantifies the rates of solvent deuterium exchange into the amide moieties of the protein backbone.⁶¹⁻⁶² The HDX rate of a given amide is highly sensitive to solvent accessibility and to the local hydrogen bonding environment. In order for HDX to occur at a given amide, structured regions of the protein must dynamically sample open conformations where intramolecular hydrogen bonds are broken and the backbone amide is exposed to solvent. For data collection, the exchange reaction is acid quenched at desired time points, the sample is proteolyzed, and the resulting proteolytic peptides are subjected to LC-MS. The mass increase of individual peptides (caused by solvent deuterium uptake) is then determined as a function of time to elucidate the HDX rate for that peptide. Thus, HDX-MS provides a direct measurement of peptide-level conformational dynamics across the entire enzyme structure. Moreover, the experiment is conducted under near native conditions with tiny amounts of material and without the requirement for expensive, laborious, and/or functionally disruptive site-specific labeling schemes. The HDX reaction can then be repeated in the presence of different ligands or with different mutant enzymes to determine how the perturbation alters the exchange properties of the enzyme. In this manner, substrate binding

sites, allosteric networks, and intramolecular conformational changes can be systematically discovered and characterized.

Draft

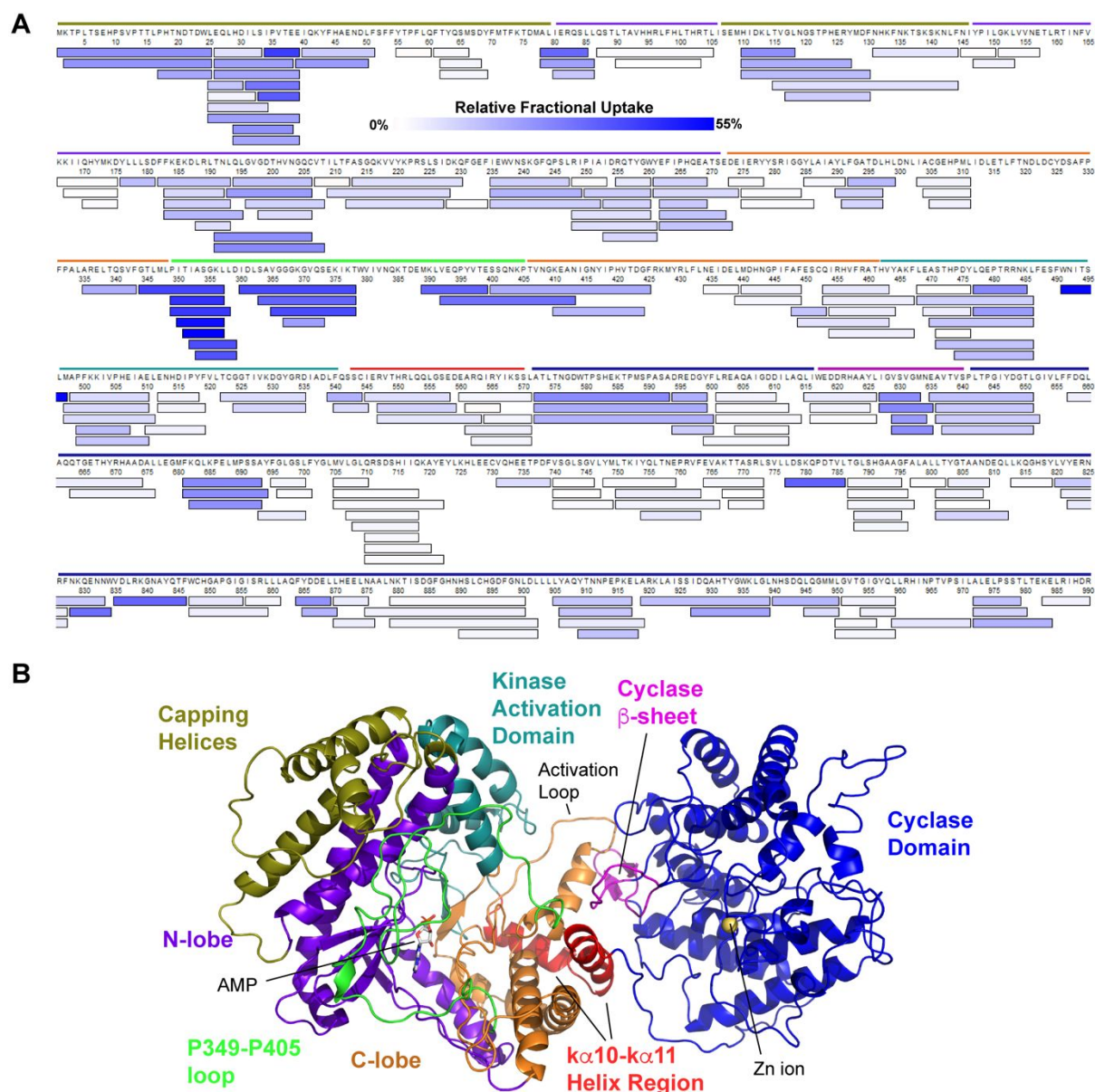


Figure 8. Hydrogen-deuterium exchange mass spectrometry (HDX-MS) of HaIM2 reveals dynamic structural elements. A) Coverage map showing peptides obtained by on-line cleavage of HaIM2 with pepsin following solvent deuterium exchange. The blue color of each peptide indicates the fractional deuterium uptake relative to an undeuterated control as determined by mass spectrometry. The colored bars above the HaIM2 amino acid sequence denote the functional domains of the enzymes as deduced from multiple amino acid sequence alignments and comparison to the high-resolution X-ray crystal structure of the cytolysin synthetase (CyIM). B) Homology model of HaIM2 with functional domains colored as in panel A. Data have been reproduced with permission from reference 40.

We developed an HDX-MS workflow for HalM2 that reproducibly generates over 200 HalM2-derived peptides, provides nearly 90% sequence coverage, and allows measurement of deuterium uptake differences as small as 0.4 Da at the 99% confidence interval (Figure 8A).⁴⁰⁻⁴² The most dynamic regions of the free enzyme (e.g. highest deuterium uptake) include the *N*-terminal capping helices, the interface between the kinase activation domain and the activation loop, the interface between the cyclase domain and the dehydrase *C*-lobe, and a large loop spanning HalM2 residues P349-P405 (Figure 8B). Upon binding to the HalA2 precursor peptide and the non-hydrolyzable ATP analogue AMP-PNP, a marked structural organization occurred within several regions of the enzyme (Figure 9). These included two loop elements in the *N*-terminal capping domain (E39-L50 and H110-P123). The sequence corresponding to H110-P123 is not ordered in the CylM crystal structure.^{40, 42, 63} Replacement of segments of the H110-P123 region with unstructured Gly-Ser linkers strongly reduced the HalA2 binding affinity (Figure 10A).⁴⁰ Moreover, photochemical crosslinking studies suggested direct contact between the HalA2 leader peptide and the E39-L50 element.⁶³ Together, these data indicate that the capping helices – which are unique to LanM enzymes – play an important role in precursor peptide binding. It should be noted that, prior to this HDX-MS work, the location of the leader peptide binding site in LanM enzymes was not known, highlighting the potential of HDX-MS for revealing functionally important enzyme-peptide interactions in RiPP biosynthetic systems. In addition, a putative β -stranded element (M389-Y396) and a conserved Thr387/Asp387 dipeptide motif in the disordered P349-P405 loop also play a role in defining the HalA2 binding site. Mutation of either of these elements led to a 5-fold decrease in HalA2 binding affinity and prevented the otherwise strong structural organization in the H110-P123 region.⁴² The coupled HDX-MS changes in the capping helices and P349-P405 loop suggest that these two elements directly interact. This conclusion was supported by 1 μ s MD simulations of a HalM2 homology model, which indicated formation of extensive hydrophobic contacts between the capping helices and the P349-P405 loop.⁴² Moreover, replacement of M389-Y396 with a Gly-Ser linker (the HalM2_{GS389} variant) led to drastic increases in the production of phosphorylated intermediates, suggesting that the normally efficient coupling of phosphorylation and elimination in the dehydratase active site is lost in this variant (Figure 10B).⁴² This result provides additional support that the disordered P349-P405 loop plays an integral role in enforcing catalytically competent conformations of the dehydratase domain upon HalA2 binding. This HalM2_{GS389} variant also catalyzes installation of the four thioether rings

of HalA2 in an entirely different order than wild type HalM2,⁴² suggesting that P349-P405 loop also plays an additional important role in the cyclization reactions.

HalA2 binding also triggered significantly less deuterium uptake in the β -sheet region of the cyclase at the interface of the cyclase and dehydratase domains (Figure 9B). On the basis of its resemblance to the winged helix-turn-helix peptide binding motif that is widely distributed in RiPP biosynthetic enzymes (referred to as the RiPP recognition element),⁶⁴ this β -sheet (HalM2 residues I616-S640) was initially proposed to serve as the primary precursor peptide binding site in LanM enzymes.³⁰ Indeed, the structural organization of this element induced by HalA2 binding initially appeared to confirm this putative function. Curiously, however, replacement of the third strand of this β -sheet with an unstructured Gly-Ser linker (the HalM2_{GS635} mutant) had no effect on the HalA2 binding affinity.⁴⁰ This finding is consistent with the primary HalA2 leader peptide binding site being confined to the *N*-terminal dehydratase domain. This claim is supported by biochemical studies of *C*-terminally truncated LanM variants that lack the β -sheet (as well as the rest of the cyclase domain), but that are still highly competent dehydratase enzymes.^{30, 39, 63, 65-66} Instead, the HalM2_{GS635} mutant suffered from reduced cyclization rates and less control over the order of the cyclization events,⁴² suggesting that the β -sheet may play a role in core peptide docking into the cyclase active site (Figure 10B). Relative comparison of the deuterium uptake in the β -sheets of the HalM2:AMP-PNP Michaelis complexes with full length HalA2 and the HalA2 leader peptide support this role. Namely, when only the HalA2 leader peptide is bound, the extent of structural organization in the β -sheet is reduced, providing support for a direct interaction between the core peptide and the β -sheet.⁴⁰

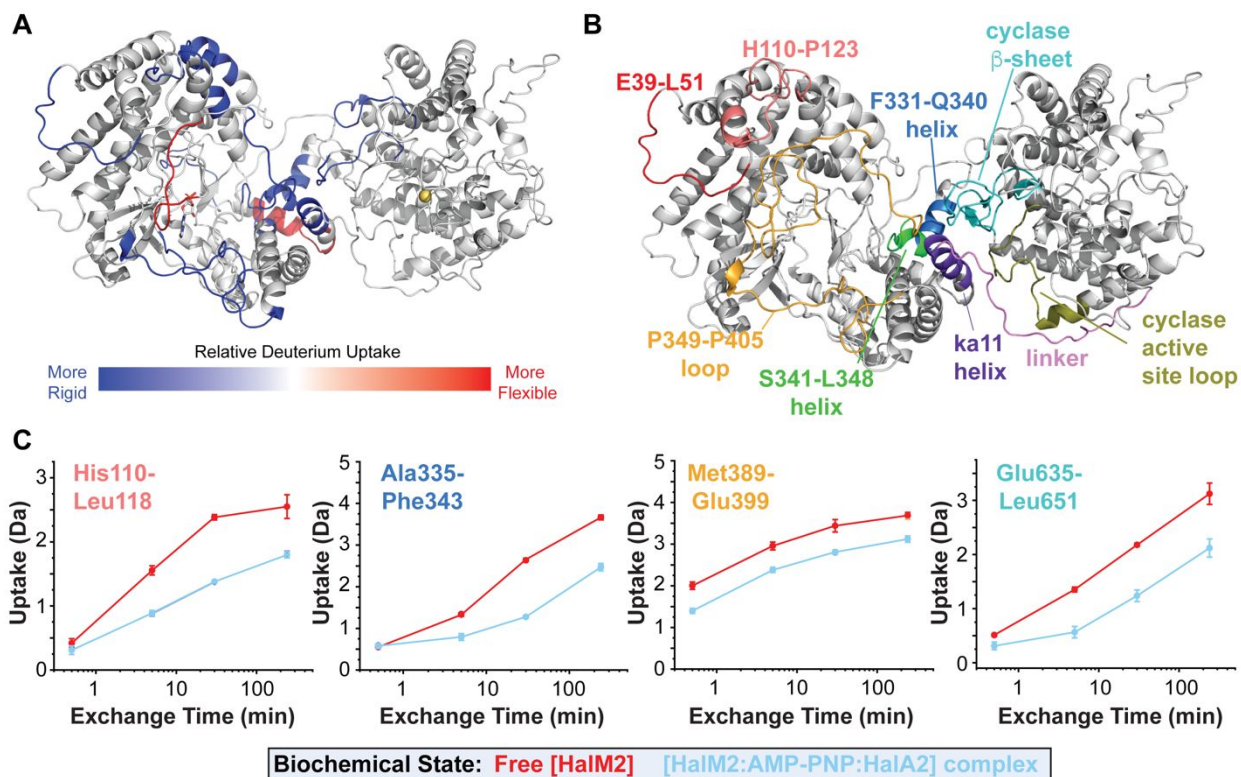


Figure 9. Differential HDX-MS in the presence of ligands reveals functionally relevant dynamic elements. A) Binding of the HalA2 precursor peptide and the non-hydrolyzable ATP analogue, AMP-PNP, result in rigidification (blue) and loosening (red) of local HalM2 structure. B) Regions of HalM2 that undergo the strongest rigidification are located in dynamic loop elements (E39-L51, H110-P123, P349-P405) and the interface of the dehydratase and cyclase domains (F331-Q340 helix, S341-L348 helix, cyclase β -sheet). C) Deuterium uptake plots for peptides derived from the *N*-terminal capping domain (H110-L118), the central helical region (A335-F343), the P349-P405 loop (M389-E399), and cyclase β -sheet (E365-L651). Data were measured in triplicate for the free enzyme and HalM2:AMP-PNP:HalA2 complex. Data have been reproduced with permission from reference 40.

Finally, HalA2 binding reduced deuterium uptake in a conserved helical region in the core of the enzyme spanning residues F331-L348 in the dehydratase domain (Figure 9B). Replacement of these helices with unstructured Gly-Ser linkers exerted severe effects on HalM2 activity (Figure 10A). Namely, HalM2_{GS341} (replacement of S341-L348) was nearly devoid of activity and catalyzed only a single phosphorylation. The activity of HalM2_{GS331} (replacement of F331-Q340) was likewise disrupted, with this enzyme only generating partially modified HalA2 intermediates at a much-reduced rate. Both HalM2_{GS331} and HalM2_{GS341} variants bound to HalA2 with near wild

type binding affinities,⁴⁰ suggesting that the enzymes are still properly folded, and providing additional support that the primary binding site for the HalA2 precursor peptide involves the capping helices with assistance from the P349-P405 loop (both of which remained intact in these variants). The HDX-MS properties of the HalM2_{GS331} and HalM2_{GS341} variants were also interesting and contrasted starkly with the other variants. In the presence of HalA2, both variants underwent moderate to significant structural relaxation in many of the HalM2 elements that normally become organized upon HalA2 binding.⁴² Our working model to explain these observations is that HalA2 binding triggers a conformational change in the F331-L348 helical region through allosteric effects that is required for high level enzyme activity.

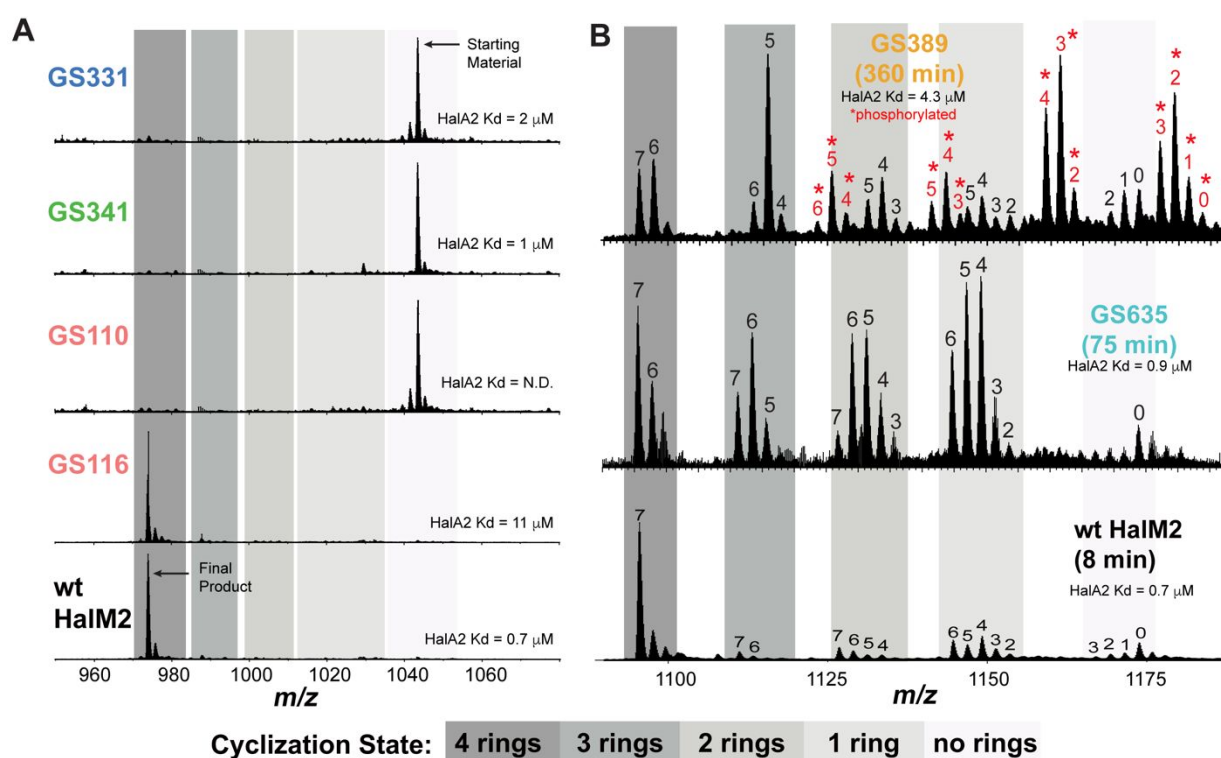


Figure 10. Enzymatic activity of HalM2 variant enzymes containing Gly-Ser linker replacements in dynamic structural elements. A) Replacement of F331-Q340 (GS331) and S341-L348 (GS341) with Gly-Ser linkers result in enzymes with severely impaired activity, but near wild type HalA2 binding affinity. In contrast, HalA2 binding to the H110-T115 mutant (GS110) could not be detected, while mutation to the adjacent region V116-P123 (GS116) reduced HalA2 binding affinity 16-fold without strongly affecting catalysis. B) The Gly-Ser replacement of M389-E399 (GS389) in the large P349-P405 loop resulted in the accumulation of phosphorylated intermediates suggesting a severely disrupted dehydratase active site structure, where the

normally efficient coupling of phosphoryl transfer and elimination is perturbed. Mutation to the cyclase β -sheet (GS635) significantly reduced the rate of cyclization catalysis and also resulted in un-natural thioether topologies. The HalA2 9⁺ and 8⁺ ions are shown in panels A and B, respectively.

Cumulatively, the HDX-MS analysis on HalM2⁴⁰ and its variant enzymes⁴² revealed that many previously overlooked, dynamic structural elements play important roles in HalM2 function. It should be emphasized that these dynamic elements contain none of the conserved residues involved in dehydration or cyclization catalysis,^{30, 44-45} illustrating the power of HDX-MS for revealing functionally important biophysical interactions. These data provide additional strong support for a LanM mechanistic model that is critically reliant on enzyme conformational changes and enzymes-peptide interactions.

6. Investigating native HalM2 structures and non-covalent interactions in the gas phase with native ion mobility mass spectrometry (IM-MS)

HDX-MS is a highly sensitive and powerful technique for revealing local structural dynamics. On the basis of HDX-MS data alone, however, it is generally not possible to assess changes in the tertiary structure of the enzyme, which are likewise expected to be important and mechanistically informative in LanM systems. More generally, many RiPP natural products, including the class I lanthipeptides, are biosynthesized by protein complexes.⁶⁷ The nature of the protein-protein and protein-peptide interactions in these complexes, and their relationship to function is not well understood. To address this need in the biophysical characterization of RiPP systems and to bridge the gap between local changes in secondary structure (HDX-MS) and global conformational changes, we have developed and applied native electrospray ionization MS approaches to investigate the conformational landscapes (tertiary structure) and intermolecular interactions (quaternary structure) in LanM:LanA systems.

Native mass spectrometry refers to a set of approaches whereby proteins or protein complexes are transferred from aqueous solution into the gas phase in a manner that preserves native conformations and non-covalent interactions.⁶⁸⁻⁶⁹ In native MS, proteins are electrosprayed from aqueous solutions containing a volatile electrolyte (typically ammonium acetate, pH ~ 6.5-7.5) using nanospray emitters with a small diameter orifice (< 1 μ M). The small orifice reduces the

size of the initial ESI droplets such that efficient protein ion desolvation occurs in the source without extensive droplet heating and/or the application of the strong electric fields typically used in ESI-MS (3-5 kV). Along with careful control of the gas pressures and ion kinetic energies in the MS instrument, these features ensure that the intra- and intermolecular non-covalent interactions that define protein tertiary and quaternary structure remain intact in the gas phase. Once in the gas phase, the conformational landscape of the protein ions can be interrogated using ion mobility (IM), which separates ions on the basis of their shapes (conformations).⁷⁰⁻⁷³ In IM separations, protein ions are transmitted at low kinetic energy through a chamber filled with buffer gas (usually nitrogen or helium). Low energy collisions between the protein ion and the buffer gas determine the drift time of the protein ion through the chamber. Protein conformations that are more closed/compact have smaller IM drift times than conformations that are more open/extended. Importantly, the drift times measured by IM-MS can be used to calculate protein ion collisional cross sections (CCS) that can be compared directly with CCS values calculated from high-resolution structures or homology models to support the existence of native structures in the gas phase.

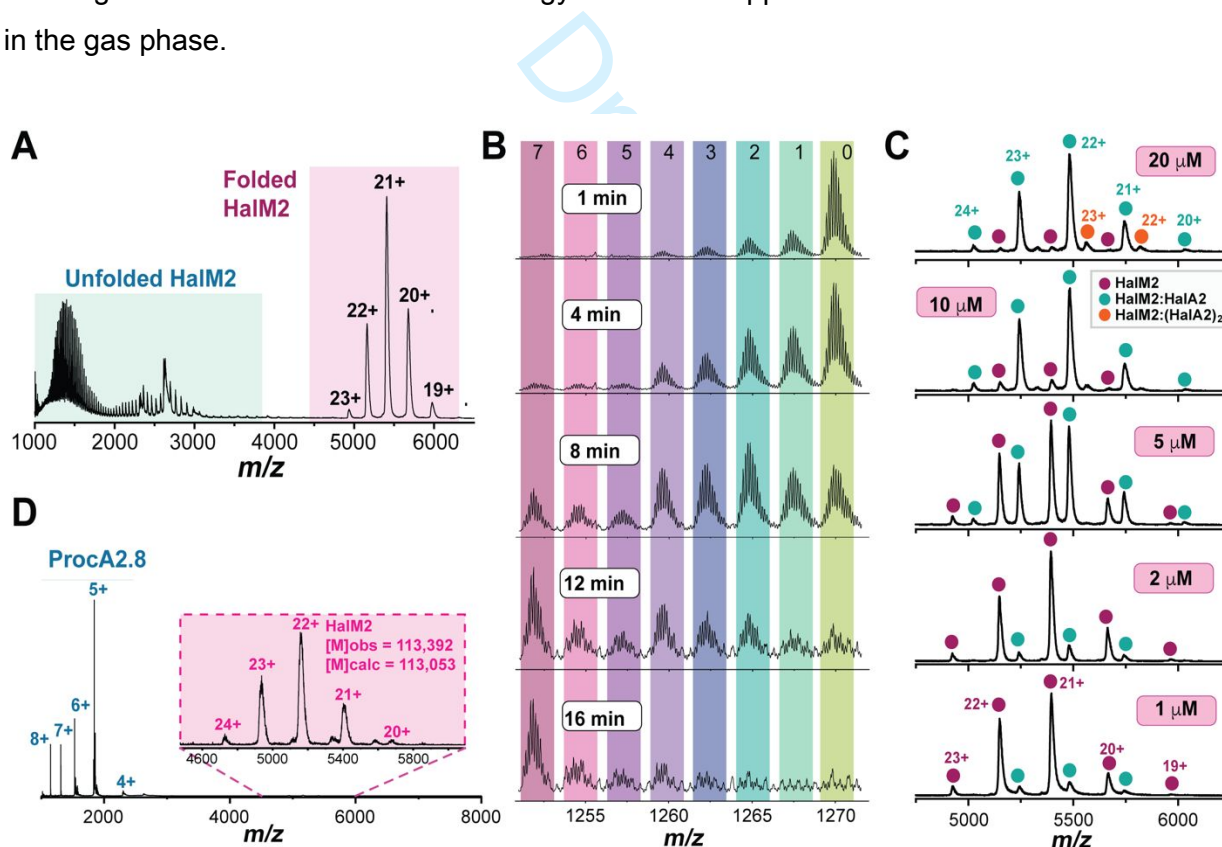


Figure 11. Native mass spectrometry characterization of HalM2. A) Using gentle instrument conditions, HalM2 can be ionized and transferred to the gas phase in a folded conformation. B) HalM2 catalyzes HalaA2 dehydration in the ESI source under the conditions used for native MS.

C) Native intermolecular contacts are maintained between HalM2 and HalA2 in the gas phase. The saturation of MS signals corresponding to the HalM2:HalA2 complex occurs with a HalA2 binding affinity that closely matches the value measured in solution titration experiments. D) HalM2 does not form a stable gas phase complex with the ProcA2.8 precursor peptide, again suggesting native specific interactions with HalA2 in panel C. Data have been reproduced with permission from reference 43.

Native MS analysis of HalM2⁴³ revealed a set of ions centered around $m/z = 5500$ corresponding to natively folded HalM2 (Figure 11A), as well as more highly charged HalM2 ions that correspond to HalM2 conformations that partially unfold during the ionization process. The shift in charge state distribution to lower values and the broadening of m/z signals are hallmarks of natively folded protein ions. The lower charge state distribution indicates that many potential ionization sites are shielded from protonation by the folded conformation of the protein. The broadening of the m/z signals suggests that the protein remains partially solvated in the gas phase and reflects the gentle ionization conditions used in the electrospray source. Several experiments were performed to assess whether the 19-23⁺ ions represented natively folded HalM2 conformations. First, the catalytic activity of HalM2 was measured in the mass spectrometer under the instrumental conditions used to collect the native MS data (Figure 11B). This experiment indicated that HalM2 catalyzed the dehydration of HalA2 with similar kinetics as was observed in the LC-ESI-MS assays,^{38, 40, 42} and also raised the possibility of using ESI-MS to perform continuous kinetic assays of LanM (and other RiPP biosynthetic) enzymes. Second, we investigated the binding affinity to HalA2 by varying the concentration of HalA2 in the reaction mixture (Figure 11C). This experiment resulted in a separate set of MS signals corresponding to the HalM2:HalA2 complex. Quantitation of the relative abundances of the HalM2 and HalM2:HalA2 ion signals allowed us to measure a binding constant for HalA2 that closely resembled values measured in solution.^{38, 40, 52} This important result provides strong support that the HalM2 and HalM2:HalA2 ion ratios measured in the gas phase reflect ratios that existed in solution, and suggested that native non-covalent contacts are retained between HalM2 and HalA2 in the gas phase. Moreover, small quantities of a complex with HalM2:HalA2 stoichiometry of 1:2 could also be detected in the native MS signals, suggesting that HalM2 may possess a second binding site for HalA2. This result illustrates the ease and resolution with which native MS can discriminate the stoichiometries of protein complexes present in a reaction mixture, which should prove useful in the characterization of other RiPP systems. Finally, HalM2 was unable to form a

stable gas phase complex with ProcA2.8 (a non-cognate precursor peptide), providing additional support that the observed interactions between HalM2 and HalA2 are the result of specific intermolecular binding interactions (Figure 11D).

The studies described above provided strong evidence that HalM2 and the HalM2:HalA2 complex maintain native conformations in the gas phase. To probe the conformational landscapes of these ions in more detail and to assess the effects of HalA2 binding on the tertiary structure of HalM2, we turned to ion mobility experiments (Figure 12A).⁴³ Interestingly, investigation of the drift time distributions for HalM2 showed the existence of two major gas phase populations – a more compact conformation (drift time = 9.19 ms) and a more open conformation (drift time = 10.73 ms). The collisional cross sections calculated from the measured drift times (63.1 and 66.9 nm², respectively) are in excellent agreement with the CCS value calculated from the HalM2 homology model (64.2 nm²),⁴² providing further evidence that the gas phase conformations reflect native solution phase structures. To ensure that the observed bimodal HalM2 conformational distribution was not the result of gas phase unfolding, we systematically varied the gas pressures and ion kinetic energies in the mass spectrometer in an attempt to unfold HalM2 through collisional activation processes. We found that the relative abundances of the open/closed HalM2 conformations were stable over a large range of gentle MS conditions, suggesting that the observed ion mobility distributions reflect the native conformational landscape of the enzyme in solution. Upon binding to either the HalA2 leader peptide or to the full length HalA2, the difference in CCS between the open and closed conformations decreases, suggesting that peptide binding is stabilizing a more defined set of conformations (Figure 12A-C). This observation is consistent with the conformational selection model for LanM enzymes proposed previously in the context of LctM^{46, 48} and HalM2.⁵² Intriguingly, the full-length peptide has a more pronounced effect on the HalM2 conformational distribution than the leader peptide, suggesting that interactions with the core peptide may be influencing the global tertiary structure of HalM2. To provide additional evidence that the HalA2 core peptide is indeed engaging in specific intermolecular interactions with HalM2, we performed collision induced unfolding studies of HalM2, and the HalM2:HalA2 and HalM2:HalA2_{leader} complexes (Figure 12D-F). In this experiment, natively folded ions are subjected to incremental increases in kinetic energy in an argon-filled trap prior to ion mobility separation.⁷⁴ Collisions with argon deposit internal energy into the protein ions that trigger ion heating and protein denaturation that is detectable by ion mobility. This experiment clearly showed that full length HalA2 stabilized the native HalM2 fold to a greater extent than the HalA2

leader peptide (Figure 12G), providing evidence for the existence of additional (stabilizing) non-covalent contacts between the HalA2 core peptide and HalM2.

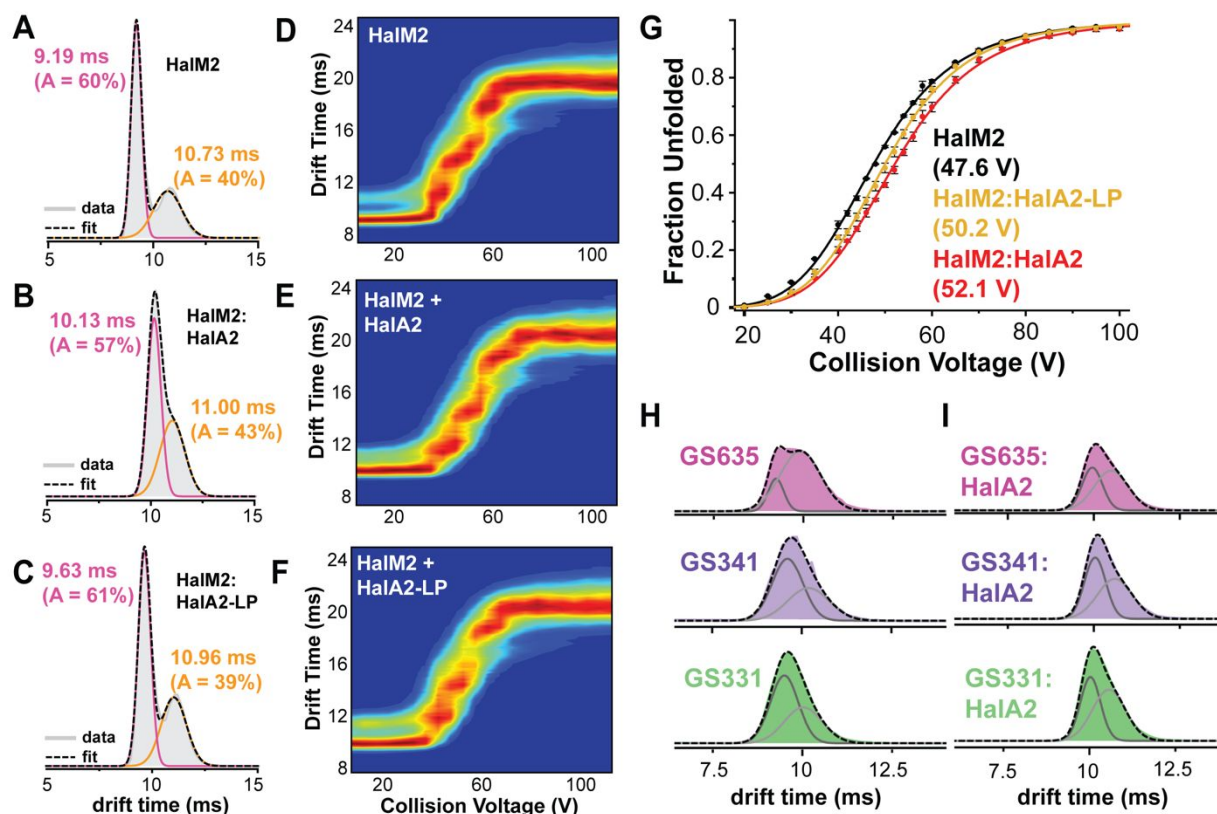



Figure 12. Investigating HalM2 conformational landscape with ion mobility mass spectrometry. Ion mobility drift time distributions for the 22⁺ ions of natively folded HalM2 (panel A), HalM2:HalA2 (B), and HalM2:HalA2_{Leader_Peptide} (C). Two major conformational populations were observed. The distribution between the two conformations was altered by peptide binding. Collision induced unfolding (CIU) of HalM2 (D), HalM2:HalA2 (E), and HalM2:HalA2_{Leader_Peptide} (F) was triggered by collisional activation with argon and monitored by ion mobility. G) The spectral means at each collision voltage were extracted from D-F and fitted to estimate the CIU₅₀ value for each ion. Full length HalA2 stabilized HalM2 to a greater extent than the HalA2 leader peptide, suggesting stable interactions between HalM2 the HalA2 core peptide. Ion mobility studies of HalM2 variant enzymes in the absence (H) and presence (I) of HalA2 suggest that the dehydratase F331-Q340 and S341-L348 α -helices and cyclase β -sheet play important roles in defining the conformational landscape. Data have been reproduced with permission from reference 43.

Finally, characterization of the ion mobility properties of the HalM2 variant enzymes discussed above in the context of the HDX-MS studies revealed critical roles for the dehydratase helical region (residues F331-L348) and cyclase β -sheet (residues I616-S640) in governing the conformational distribution between the open/closed conformations. Namely, in the HalM2_{GS331}, HalM2_{GS340}, and HalM2_{GS635} variants, the open conformation becomes more populated in the free enzymes (Figure 12H). Moreover, the conformational landscape of the free enzyme becomes less sensitive to HalA2 binding (Figure 12I). Importantly, as revealed by titration experiments, these HalM2 variants each bind to HalA2 with near wild type binding affinity.⁴⁰ Thus, the ion mobility data suggests that these variants are defective in a HalA2 binding-induced conformational change involving the conserved F331-L348 α -helices and the β -sheet at the interface of the dehydratase and cyclase domains. The results further underscore the importance of these elements to the structure and function of HalM2.

7. Conclusions and Future Perspectives



Cumulatively, our studies on HalM2 have enabled some of the most quantitative descriptions of RiPP biosynthetic enzyme function reported to date, and have allowed us to untangle the complex networks of chemical reactions and biomolecular interactions that typify these systems. The mass spectrometry-based approaches highlighted in this review have provided unique insights into the relationship between the structural dynamics and function of the HalM2:HalA2 system that were not accessible by other methods. The data have consistently illustrated that conformational changes and intermolecular protein-peptide interactions play an absolutely essential role in defining the important functional properties of HalM2. We suspect that similar “biophysical” process will be critically important in many other RiPP biosynthetic systems, and may ultimately represent the unifying biosynthetic paradigm in this class of natural products. As such, we expect that continued application of MS-based approaches will illuminate functional heterogeneity and biophysical mechanisms in the myriad other RiPP biosynthetic enzymes that await detailed mechanistic characterization. It should also be emphasized that all of our MS data on the HalM2:HalA2 system were collected on the same commercially available, versatile, and user-friendly MS instrument (a Waters Synapt G2-Si). Thus, the comprehensive, general experimental approaches we have developed should be accessible to many other researchers in the RiPP field.

To date, much of the research in the RiPP biosynthesis field has focused on the discovery and characterization of structurally novel RiPPs, and on assessing the capacity of RiPP biosynthetic enzymes for the engineering of novel, post-translationally modified peptides.¹⁻² These efforts have provided a rapidly expanding set of enzymes, peptides, and experimental/computational tools for engineering applications. However, aside from a few notable exceptions,⁷⁵⁻⁸² molecular mechanistic details of the enzyme-peptide interactions and structural properties that govern biosynthesis remain poorly understood, difficult to predict, and difficult to measure. A thorough understanding of enzyme-peptide interactions and of RiPP biosynthetic mechanisms will be necessary for the development of strategies to engineer novel RiPPs with novel functions using renewable enzymatic and cell-based resources.

In lieu of traditional high-resolution structural biology approaches to elucidate enzyme-peptide interactions, which often prove challenging to apply to RiPP systems, our work on HalM2 has provided several alternative MS-based methods for direct interrogation of peptide binding modes, allosteric networks, and dynamic conformational changes. An intriguing aspect of the HalM2:HalA2 system is that most of the dynamic structural elements that are important for function (as assessed by HDX-MS, site-directed mutagenesis, and kinetic assays) involve conserved local structural elements rather than absolutely conserved amino acid sequences. Moving forward, it will be interesting to investigate whether the conformational dynamics identified in HalM2 are conserved across the LanM family, or whether the functionally important conformational dynamics have evolved in a system-dependent manner that ultimately imparts system-specific functional properties. Secondly, as our native IM-MS measurements indicate, both the leader and core peptide portions of the HalA2 precursor influence the tertiary structure of HalM2, providing direct evidence that intermolecular interactions with the core peptide can influence the structure (and perhaps also the function) of HalM2. The influence of the HalA2 core peptide on the tertiary structure of the synthetase is particularly interesting. Using partially-modified HalA2 analogues in combination with HDX-MS and native MS, it may now be possible to directly test whether post-translational modification of HalA2 alters the conformational properties of HalM2 in a systematic fashion. These types of studies are pertinent to all iteratively-acting RiPP biosynthetic enzymes, yet have remain experimentally inaccessible by more traditional biophysical techniques. It is our prediction that the impressive resolving power and sensitivity of mass spectrometry based approaches will continue to make important contributions to our understanding of lanthipeptide and RiPP biosynthesis.

Draft

References

1. Annison, P. G.; Bibb, M. J.; Bierbaum, G.; Bowers, A. A.; Bugni, T. S.; Bulaj, G.; Camarero, J. A.; Campopiano, D. J.; Challis, G. L.; Clardy, J.; Cotter, P. D.; Craik, D. J.; Dawson, M.; Dittmann, E.; Donadio, S.; Dorrestein, P. C.; Entian, K. D.; Fischbach, M. A.; Garavelli, J. S.; Goransson, U.; Gruber, C. W.; Haft, D. H.; Hemscheidt, T. K.; Hertweck, C.; Hill, C.; Horswill, A. R.; Jaspars, M.; Kelly, W. L.; Klinman, J. P.; Kuipers, O. P.; Link, A. J.; Liu, W.; Marahiel, M. A.; Mitchell, D. A.; Moll, G. N.; Moore, B. S.; Müller, R.; Nair, S. K.; Nes, I. F.; Norris, G. E.; Olivera, B. M.; Onaka, H.; Patchett, M. L.; Piel, J.; Reaney, M. J.; Rebuffat, S.; Ross, R. P.; Sahl, H. G.; Schmidt, E. W.; Selsted, M. E.; Severinov, K.; Shen, B.; Sivonen, K.; Smith, L.; Stein, T.; Süßmuth, R. D.; Tagg, J. R.; Tang, G. L.; Truman, A. W.; Vederas, J. C.; Walsh, C. T.; Walton, J. D.; Wenzel, S. C.; Willey, J. M.; van der Donk, W. A., Ribosomally synthesized and post-translationally modified peptide natural products: overview and recommendations for a universal nomenclature. *Nat. Prod. Rep.* **2013**, *30* (1), 108-160.
2. Montalban-Lopez, M.; Scott, T. A.; Ramesh, S.; Rahman, I. R.; van Heel, A. J.; Viel, J. H.; Bandarian, V.; Dittmann, E.; Genilloud, O.; Goto, Y.; Grande Burgos, M. J.; Hill, C.; Kim, S.; Koehnke, J.; Latham, J. A.; Link, A. J.; Martinez, B.; Nair, S. K.; Nicolet, Y.; Rebuffat, S.; Sahl, H. G.; Sareen, D.; Schmidt, E. W.; Schmitt, L.; Severinov, K.; Süßmuth, R. D.; Truman, A. W.; Wang, H.; Weng, J. K.; van Wezel, G. P.; Zhang, Q.; Zhong, J.; Piel, J.; Mitchell, D. A.; Kuipers, O. P.; van der Donk, W. A., New developments in RiPP discovery, enzymology and engineering. *Nat. Prod. Rep.* **2021**, *38*, 130-239.
3. Urban, J. H.; Moosmeier, M. A.; Aumüller, T.; Thein, M.; Bosma, T.; Rink, R.; Groth, K.; Zully, M.; Siegers, K.; Tissot, K.; Moll, G. N.; Prassler, J., Phage display and selection of lanthipeptides on the carboxy-terminus of the gene-3 minor coat protein. *Nat. Commun.* **2017**, *8* (1), 1500.
4. Burkhart, B. J.; Kakkar, N.; Hudson, G. A.; van der Donk, W. A.; Mitchell, D. A., Chimeric Leader Peptides for the Generation of Non-Natural Hybrid RiPP Products. *ACS Cent. Sci.* **2017**, *3* (6), 629-638.
5. Hetrick, K. J.; Walker, M. C.; van der Donk, W. A., Development and Application of Yeast and Phage Display of Diverse Lanthipeptides. *ACS Cent. Sci.* **2018**, *4* (4), 458-467.
6. Yang, X.; Lennard, K. R.; He, C.; Walker, M. C.; Ball, A. T.; Doigneaux, C.; Tavassoli, A.; van der Donk, W. A., A lanthipeptide library used to identify a protein-protein interaction inhibitor. *Nat. Chem. Biol.* **2018**, *14*, 375-380.

7. Schmitt, S.; Montalban-Lopez, M.; Peterhoff, D.; Deng, J.; Wagner, R.; Held, M.; Kuipers, O. P.; Panke, S., Analysis of modular bioengineered antimicrobial lanthipeptides at nanoliter scale. *Nat. Chem. Biol.* **2019**, *15* (5), 437-443.
8. Zhao, X.; Cebrian, R.; Fu, Y.; Rink, R.; Bosma, T.; Moll, G. N.; Kuipers, O. P., High-Throughput Screening for Substrate Specificity-Adapted Mutants of the Nisin Dehydratase NisB. *ACS Synth. Biol.* **2020**, *9* (6), 1468-1478.
9. Medema, M. H.; Blin, K.; Cimermancic, P.; de Jager, V.; Zakrzewski, P.; Fischbach, M. A.; Weber, T.; Takano, E.; Breitling, R., antiSMASH: rapid identification, annotation and analysis of secondary metabolite biosynthesis gene clusters in bacterial and fungal genome sequences. *Nuc. Acids Res.* **2011**, *39* (Web Server issue), W339-W346.
10. de Jong, A.; van Heel, A. J.; Kok, J.; Kuipers, O. P., BAGEL2: mining for bacteriocins in genomic data. *Nuc. Acids Res.* **2010**, *38* (Web Server issue), W647-W651.
11. Tietz, J. I.; Schwalen, C. J.; Patel, P. S.; Maxson, T.; Blair, P. M.; Tai, H. C.; Zakai, U. I.; Mitchell, D. A., A new genome-mining tool redefines the lasso peptide biosynthetic landscape. *Nat. Chem. Biol.* **2017**, *13* (5), 470-478.
12. Repka, L. M.; Chekan, J. R.; Nair, S. K.; van der Donk, W. A., Mechanistic Understanding of Lanthipeptide Biosynthetic Enzymes. *Chem. Rev.* **2017**, *117* (8), 5457-5520.
13. Zhang, Q.; Doroghazi, J. R.; Zhao, X.; Walker, M. C.; van der Donk, W. A., Expanded natural product diversity revealed by analysis of lanthipeptide-like gene clusters in actinobacteria. *Appl. Environ. Microbiol.* **2015**, *81* (13), 4339-4350.
14. Walker, M. C.; Eslami, S. M.; Hetrick, K. J.; Ackenhusen, S. E.; Mitchell, D. A.; van der Donk, W. A., Precursor peptide-targeted mining of more than one hundred thousand genomes expands the lanthipeptide natural product family. *BMC genomics* **2020**, *21* (1), 387-403.
15. Mohr, K. I.; Volz, C.; Jansen, R.; Wray, V.; Hoffmann, J.; Bernecker, S.; Wink, J.; Gerth, K.; Stadler, M.; Muller, R., Pinensins: the first antifungal lantibiotics. *Angew. Chem. Int. Ed.* **2015**, *54* (38), 11254-11258.
16. Ferir, G.; Petrova, M. I.; Andrei, G.; Huskens, D.; Hoorelbeke, B.; Snoeck, R.; Vanderleyden, J.; Balzarini, J.; Bartoschek, S.; Bronstrup, M.; Sussmuth, R. D.; Schols, D., The lantibiotic peptide labyrinthopeptin A1 demonstrates broad anti-HIV and anti-HSV activity with potential for microbicidal applications. *PloS one* **2013**, *8* (5), e64010.
17. Cox, C. R.; Coburn, P. S.; Gilmore, M. S., Enterococcal cytolysin: a novel two component peptide system that serves as a bacterial defense against eukaryotic and prokaryotic cells. *Curr. Protein Pept. Sci.* **2005**, *6* (1), 77-84.

18. Kodani, S.; Hudson, M. E.; Durrant, M. C.; Buttner, M. J.; Nodwell, J. R.; Willey, J. M., The SapB morphogen is a lantibiotic-like peptide derived from the product of the developmental gene ramS in *Streptomyces coelicolor*. *Proc. Natl Acad. Sci. U.S.A.* **2004**, *101* (31), 11448-11453.
19. Meindl, K.; Schmiederer, T.; Schneider, K.; Reicke, A.; Butz, D.; Keller, S.; Guhring, H.; Vertesy, L.; Wink, J.; Hoffmann, H.; Bronstrup, M.; Sheldrick, G. M.; Sussmuth, R. D., Labyrinthopeptins: a new class of carbacyclic lantibiotics. *Angew. Chem. Int. Ed.* **2010**, *49* (6), 1151-1154.
20. Xu, M.; Zhang, F.; Cheng, Z.; Bashiri, G.; Wang, J.; Hong, J.; Wang, Y.; Xu, L.; Chen, X.; Huang, S. X.; Lin, S.; Deng, Z.; Tao, M., Functional Genome Mining Reveals a Class V Lanthipeptide Containing a d-Amino Acid Introduced by an F420 H₂ -Dependent Reductase. *Angew. Chem. Int. Ed.* **2020**, *59*, 18029-18035.
21. Zhang, Q.; Yu, Y.; Velasquez, J. E.; van der Donk, W. A., Evolution of lanthipeptide synthetases. *Proc. Natl Acad. Sci. U.S.A.* **2012**, *109* (45), 18361-18366.
22. Garg, N.; Salazar-Ocampo, L. M.; van der Donk, W. A., In vitro activity of the nisin dehydratase NisB. *Proc. Natl Acad. Sci. U.S.A.* **2013**, *110* (18), 7258-7263.
23. Li, B.; Yu, J. P.; Brunzelle, J. S.; Moll, G. N.; van der Donk, W. A.; Nair, S. K., Structure and mechanism of the lantibiotic cyclase involved in nisin biosynthesis. *Science* **2006**, *311* (5766), 1464-1467.
24. Xie, L.; Miller, L. M.; Chatterjee, C.; Averin, O.; Kelleher, N. L.; van der Donk, W. A., Lacticin 481: In vitro reconstitution of lantibiotic synthetase activity. *Science* **2004**, *303*, 679-681.
25. Goto, Y.; Li, B.; Claesen, J.; Shi, Y.; Bibb, M. J.; van der Donk, W. A., Discovery of unique lanthionine synthetases reveals new mechanistic and evolutionary insights. *PLoS Biol.* **2010**, *8* (3), e1000339.
26. Ortiz-Lopez, F. J.; Carretero-Molina, D.; Sanchez-Hidalgo, M.; Martin, J.; Gonzalez, I.; Roman-Hurtado, F.; de la Cruz, M.; Garcia-Fernandez, S.; Reyes, F.; Deisinger, J. P.; Muller, A.; Schneider, T.; Genilloud, O., Cacaoidin, First Member of the New Lanthidin RiPP Family. *Angew. Chem. Int. Ed.* **2020**, *59* (31), 12654-12658.
27. Kloosterman, A. M.; Cimermancic, P.; Elsayed, S. S.; Du, C.; Hadjithomas, M.; Donia, M. S.; Fischbach, M. A.; van Wezel, G. P.; Medema, M. H., Expansion of RiPP biosynthetic space through integration of pan-genomics and machine learning uncovers a novel class of lanthipeptides. *PLoS Biol.* **2020**, *18* (12), e3001026.

28. Chatterjee, C.; Miller, L. M.; Leung, Y. L.; Xie, L.; Yi, M.; Kelleher, N. L.; van der Donk, W. A., Lactacin 481 synthetase phosphorylates its substrate during lantibiotic production. *J. Am. Chem. Soc.* **2005**, *127*, 15332-15333.
29. Muller, W. M.; Schmiederer, T.; Ensle, P.; Sussmuth, R. D., In vitro biosynthesis of the prepeptide of type-III lantibiotic labyrinthopeptin A2 including formation of a C-C bond as a post-translational modification. *Angew. Chem. Int. Ed.* **2010**, *49*(13), 2436-2440.
30. Dong, S.-H.; Tang, W.; Lukk, T.; Nair, S. K.; van der Donk, W. A., The Enterococcal Cytolysin Synthetase Has an Unanticipated Lipid Kinase Fold. *eLife* **2015**, *4*:e07607.
31. Huang, C. C.; Casey, P. J.; Fierke, C. A., Evidence for a catalytic role of zinc in protein farnesyltransferase. Spectroscopy of Co²⁺-farnesyltransferase indicates metal coordination of the substrate thiolate. *J. Biol. Chem.* **1997**, *272*(1), 20-23.
32. Harris, C. M.; Derdowski, A. M.; Poulter, C. D., Modulation of the zinc(II) center in protein farnesyltransferase by mutagenesis of the zinc(II) ligands. *Biochemistry* **2002**, *41*(33), 10554-10562.
33. Wang, H.; van der Donk, W. A., Biosynthesis of the Class III Lantipeptide Catenulepeptin. *ACS Chem. Biol.* **2012**, *7*, 1529-1535.
34. Rosing, J.; Slater, E. C., The value of G degrees for the hydrolysis of ATP. *Biochim. Biophys. Acta* **1972**, *267*(2), 275-290.
35. Krenske, E. H.; Petter, R. C.; Zhu, Z.; Houk, K. N., Transition states and energetics of nucleophilic additions of thiols to substituted alpha,beta-unsaturated ketones: substituent effects involve enone stabilization, product branching, and solvation. *J. Org. Chem.* **2011**, *76*(12), 5074-5081.
36. Tang, W.; van der Donk, W. A., The sequence of the enterococcal cytolysin imparts unusual lanthionine stereochemistry. *Nat. Chem. Biol.* **2013**, *9*, 157-159.
37. Yu, Y.; Mukherjee, S.; van der Donk, W. A., Product Formation by the Promiscuous Lanthipeptide Synthetase ProcM is under Kinetic Control. *J. Am. Chem. Soc.* **2015**, *137*(15), 5140-5148.
38. Thibodeaux, C. J.; Ha, T.; van der Donk, W. A., A Price to Pay for Relaxed Substrate Specificity: A Comparative Kinetic Analysis of the Class II Lanthipeptide Synthetases, ProcM and HalM2. *J. Am. Chem. Soc.* **2014**, *136*, 17513-17529.
39. Thibodeaux, C. J.; Wagoner, J.; Yu, Y.; van der Donk, W. A., Leader Peptide Establishes Dehydration Order, Promotes Efficiency, and Ensures Fidelity During Lactacin 481 Biosynthesis. *J. Am. Chem. Soc.* **2016**, *138*(20), 6436-6444.

40. Habibi, Y.; Uggowitzer, K. A.; Issak, H.; Thibodeaux, C. J., Insights into the Dynamic Structural Properties of a Lanthipeptide Synthetase using Hydrogen-Deuterium Exchange Mass Spectrometry. *J. Am. Chem. Soc.* **2019**, *141*, 14661-14672.
41. Habibi, Y.; Thibodeaux, C. J., A Hydrogen-Deuterium Exchange Mass Spectrometry (HDX-MS) Platform for Investigating Peptide Biosynthetic Enzymes. *J. Vis. Exp.* **2020**, *159*, e61053.
42. Uggowitzer, K. A.; Habibi, Y.; Wei, W.; Moitessier, N.; Thibodeaux, C. J., Mutations in Dynamic Structural Elements Alter the Kinetics and Fidelity of the Multifunctional Class II Lanthipeptide Synthetase, HalM2 *Biochemistry* **2021**, *60*, 412-430.
43. Weerasinghe, N. W.; Habibi, Y.; Uggowitzer, K. A.; Thibodeaux, C. J., Exploring the Conformational Landscape of a Lanthipeptide Synthetase using Native Mass Spectrometry. *Biochemistry* **2021**, *60*, 1506-1519.
44. You, Y. O.; van der Donk, W. A., Mechanistic investigations of the dehydration reaction of lacticin 481 synthetase using site-directed mutagenesis. *Biochemistry* **2007**, *46* (20), 5991-6000.
45. Paul, M.; Patton, G. C.; van der Donk, W. A., Mutants of the zinc ligands of lacticin 481 synthetase retain dehydration activity but have impaired cyclization activity. *Biochemistry* **2007**, *46* (21), 6268-76.
46. Patton, G. C.; Paul, M.; Cooper, L. E.; Chatterjee, C.; van der Donk, W. A., The importance of the leader sequence for directing lanthionine formation in lacticin 481. *Biochemistry* **2008**, *47*, 7342-7351.
47. Oman, T. J.; Knerr, P. J.; Bindman, N. A.; Velasquez, J. E.; van der Donk, W. A., An engineered lantibiotic synthetase that does not require a leader peptide on its substrate. *J. Am. Chem. Soc.* **2012**, *134* (16), 6952-6955.
48. Levengood, M. R.; Patton, G. C.; van der Donk, W. A., The leader peptide is not required for post-translational modification by lacticin 481 synthetase. *J. Am. Chem. Soc.* **2007**, *129*, 10314-10315.
49. Yang, X.; van der Donk, W. A., Michael-Type Cyclizations in Lantibiotic Biosynthesis Are Reversible. *ACS Chem. Biol.* **2015**, *10*, 1234-1238.
50. McClerren, A. L.; Cooper, L. E.; Quan, C.; Thomas, P. M.; Kelleher, N. L.; van der Donk, W. A., Discovery and in vitro biosynthesis of haloduracin, a two-component lantibiotic. *Proc. Natl Acad. Sci. U.S.A.* **2006**, *103* (46), 17243-17248.

51. Cooper, L. E.; McClerren, A. L.; Chary, A.; van der Donk, W. A., Structure-activity relationship studies of the two-component lantibiotic haloduracin. *Chem. Biol.* **2008**, *15*, 1035-1045.
52. Thibodeaux, G. N.; McClerren, A. L.; Ma, Y.; Gancayco, M. R.; van der Donk, W. A., Synergistic binding of the leader and core peptides by the lantibiotic synthetase HalM2. *ACS Chem. Biol.* **2015**, *10* (4), 970-977.
53. Oman, T. J.; Lupoli, T. J.; Wang, T. S.; Kahne, D.; Walker, S.; van der Donk, W. A., Haloduracin alpha binds the peptidoglycan precursor lipid II with 2:1 stoichiometry. *J. Am. Chem. Soc.* **2011**, *133* (44), 17544-17547.
54. Lee, M. V.; Ihnken, L. A. F.; You, Y. O.; McClerren, A. L.; van der Donk, W. A.; Kelleher, N. L., Distributive and directional behavior of lantibiotic synthetases revealed by high-resolution tandem mass spectrometry. *J. Am. Chem. Soc.* **2009**, *131*, 12258-12264.
55. Mukherjee, S.; van der Donk, W. A., Mechanistic Studies on the Substrate Tolerant Lanthipeptide Synthetase ProcM. *J. Am. Chem. Soc.* **2014**, *136*, 10450-10459.
56. Hicks, L. M.; O'Connor, S. E.; Mazur, M. T.; Walsh, C. T.; Kelleher, N. L., Mass spectrometric interrogation of thioester-bound intermediates in the initial stages of epothilone biosynthesis. *Chem. Biol.* **2004**, *11* (3), 327-35.
57. Miller, L. M.; Mazur, M. T.; McLoughlin, S. M.; Kelleher, N. L., Parallel interrogation of covalent intermediates in the biosynthesis of gramicidin S using high-resolution mass spectrometry. *Protein Sci.* **2005**, *14* (10), 2702-12.
58. Li, B.; Sher, D.; Kelly, L.; Shi, Y.; Huang, K.; Knerr, P. J.; Joewono, I.; Rusch, D.; Chisholm, S. W.; van der Donk, W. A., Catalytic promiscuity in the biosynthesis of cyclic peptide secondary metabolites in planktonic marine cyanobacteria. *Proc. Natl Acad. Sci. U.S.A.* **2010**, *107*, 10430-10435.
59. Zhang, Q.; Yang, X.; Wang, H.; van der Donk, W. A., High divergence of the precursor peptides in combinatorial lanthipeptide biosynthesis. *ACS Chem. Biol.* **2014**, *9* (11), 2686-2694.
60. Tang, W.; van der Donk, W. A., Structural characterization of four prochlorosins: a novel class of lantipeptides produced by planktonic marine cyanobacteria. *Biochemistry* **2012**, *51* (21), 4271-9.
61. Konermann, L.; Pan, J.; Liu, Y. H., Hydrogen exchange mass spectrometry for studying protein structure and dynamics. *Chem. Soc. Rev.* **2011**, *40* (3), 1224-34.
62. Zhang, Z.; Smith, D. L., Determination of amide hydrogen exchange by mass spectrometry: a new tool for protein structure elucidation. *Protein Sci.* **1993**, *2* (4), 522-531.

63. Rahman, I. R.; Acedo, J. Z.; Liu, X. R.; Zhu, L.; Arrington, J.; Gross, M. L.; van der Donk, W. A., Substrate Recognition by the Class II Lanthipeptide Synthetase HalM2. *ACS Chem. Biol.* **2020**, *15*, 1473-1486.
64. Burkhart, B. J.; Hudson, G. A.; Dunbar, K. L.; Mitchell, D. A., A prevalent peptide-binding domain guides ribosomal natural product biosynthesis. *Nat. Chem. Biol.* **2015**, *11*(8), 564-570.
65. Shimafuji, C.; Noguchi, M.; Nishie, M.; Nagao, J. I.; Shioya, K.; Zendo, T.; Nakayama, J.; Sonomoto, K., In vitro catalytic activity of N-terminal and C-terminal domains in NukM, the post-translational modification enzyme of nukacin ISK-1. *J. Biosci. Bioeng.* **2015**, *120*, 624-629.
66. Ma, H.; Gao, Y.; Zhao, F.; Zhong, J., Individual catalytic activity of two functional domains of bovicin HJ50 synthase BovM. *Wei sheng wu xue bao = Acta microbiologica Sinica* **2015**, *55*(1), 50-58.
67. Sikandar, A.; Koehnke, J., The role of protein-protein interactions in the biosynthesis of ribosomally synthesized and post-translationally modified peptides. *Nat. Prod. Rep.* **2019**, *36*(11), 1576-1588.
68. Hopper, J. T.; Robinson, C. V., Mass spectrometry quantifies protein interactions-from molecular chaperones to membrane porins. *Angew. Chem. Int. Ed.* **2014**, *53*(51), 14002-14015.
69. Breuker, K.; McLafferty, F. W., Stepwise evolution of protein native structure with electrospray into the gas phase, 10(-12) to 10(2) s. *Proc. Natl Acad. Sci. U.S.A.* **2008**, *105*(47), 18145-18152.
70. Clemmer, D. E.; Hudgins, R. R.; Jarrold, M. F., Naked Protein Conformations - Cytochrome-C in the Gas-Phase. *J. Am. Chem. Soc.* **1995**, *117*(40), 10141-10142.
71. Bohrer, B. C.; Merenbloom, S. I.; Koeniger, S. L.; Hilderbrand, A. E.; Clemmer, D. E., Biomolecule analysis by ion mobility spectrometry. *Annu. Rev. Anal. Chem.* **2008**, *1*, 293-327.
72. Ruotolo, B. T.; Benesch, J. L.; Sandercock, A. M.; Hyung, S. J.; Robinson, C. V., Ion mobility-mass spectrometry analysis of large protein complexes. *Nat. Protoc.* **2008**, *3*(7), 1139-52.
73. Ruotolo, B. T.; Giles, K.; Campuzano, I.; Sandercock, A. M.; Bateman, R. H.; Robinson, C. V., Evidence for macromolecular protein rings in the absence of bulk water. *Science* **2005**, *310*(5754), 1658-1661.
74. Zhong, Y.; Han, L.; Ruotolo, B. T., Collisional and Coulombic unfolding of gas-phase proteins: high correlation to their domain structures in solution. *Angew. Chem. Int. Ed.* **2014**, *53*(35), 9209-9212.

75. Ortega, M. A.; Hao, Y.; Zhang, Q.; Walker, M.; van der Donk, W. A.; Nair, S. K., Structure and Mechanism of the tRNA-Dependent Lantibiotic Dehydratase NisB. *Nature* **2015**, *517*, 509-512.
76. Koehnke, J.; Mann, G.; Bent, A. F.; Ludewig, H.; Shirran, S.; Botting, C.; Lebl, T.; Houssen, W. E.; Jaspars, M.; Naismith, J. H., Structural analysis of leader peptide binding enables leader-free cyanobactin processing. *Nat. Chem. Biol.* **2015**, *11* (8), 558-563.
77. Grove, T. L.; Himes, P. M.; Hwang, S.; Yumerefendi, H.; Bonanno, J. B.; Kuhlman, B.; Almo, S. C.; Bowers, A. A., Structural Insights into Thioether Bond Formation in the Biosynthesis of Sactipeptides. *J. Am. Chem. Soc.* **2017**, *139*(34), 11734-11744.
78. Cogan, D. P.; Hudson, G. A.; Zhang, Z.; Pogorelov, T. V.; van der Donk, W. A.; Mitchell, D. A.; Nair, S. K., Structural insights into enzymatic [4+2] aza-cycloaddition in thiopeptide antibiotic biosynthesis. *Proc. Natl Acad. Sci. U.S.A.* **2017**, *114* (49), 12928-12933.
79. Bothwell, I. R.; Cogan, D. P.; Kim, T.; Reinhardt, C. J.; van der Donk, W. A.; Nair, S. K., Characterization of glutamyl-tRNA-dependent dehydratases using nonreactive substrate mimics. *Proc. Natl Acad. Sci. U.S.A.* **2019**, *116* (35), 17245-17250.
80. Davis, K. M.; Schramma, K. R.; Hansen, W. A.; Bacik, J. P.; Khare, S. D.; Seyedsayamdost, M. R.; Ando, N., Structures of the peptide-modifying radical SAM enzyme SuiB elucidate the basis of substrate recognition. *Proc. Natl Acad. Sci. U.S.A.* **2017**, *114* (39), 10420-10425.
81. Ghilarov, D.; Stevenson, C. E. M.; Travin, D. Y.; Piskunova, J.; Serebryakova, M.; Maxwell, A.; Lawson, D. M.; Severinov, K., Architecture of Microcin B17 Synthetase: An Octameric Protein Complex Converting a Ribosomally Synthesized Peptide into a DNA Gyrase Poison. *Mol. Cell.* **2019**, *73* (4), 749-762 e5.
82. Zhao, G.; Kosek, D.; Liu, H. B.; Ohlemacher, S. I.; Blackburne, B.; Nikolskaya, A.; Makarova, K. S.; Sun, J.; Barry Iii, C. E.; Koonin, E. V.; Dyda, F.; Bewley, C. A., Structural Basis for a Dual Function ATP Grasp Ligase That Installs Single and Bicyclic omega-Ester Macrocycles in a New Multicore RiPP Natural Product. *J. Am. Chem. Soc.* **2021**, *143* (21), 8056-8068.